Increasing Arabian dust activity and the Indian Summer Monsoon

Fabien Solmon (1), Vijayakumar S. Nair (2), Marc Mallet (3)

(1) The Abdus Salam International Center for Theoretical Physics, Strada Costiera 11, 34100 Trieste, Italy

(2) Space Physics Laboratory Vikram Sarabhai Space Centre Thiruvananthapuram Kerala, India, 695 022

(3) Laboratoire d'Aerologie CNRS, Universite Paul Sabatier, 14 av, Edouard Belin, 31400 Toulouse, France

Corresponding Author

Fabien Solmon, The Abdus Salam International Center for Theoretical Physics, ESP, Strada costiera 11 , 34100 Trieste, Italy.

+390402240206, fsolmon@ictp.it

Keywords. Arabian Dust, Decadal Trend, Indian Monsoon Precipitation, Regional climate.

Abstract.

Over the past decade, Aerosol Optical Depth (AOD) observations based on satellite and ground measurements have shown a significant increase over Arabia and the Arabian Sea, attributed to an intensification of regional dust activity. Recent studies have also suggested that west Asian dust forcing could induce a positive response of Indian monsoon precipitations on a weekly time scale. Using observations and a regional climate model including interactive slab ocean and dust aerosol schemes, the present study investigates possible climatic links between the increasing June-July-August-September (JJAS) Arabian dust activity and precipitation trends over southern India during the 2000-2009 decade. Meteorological reanalysis and AOD observations suggest that the observed decadal increase of dust activity and a simultaneous intensification of summer precipitation trend over southern India are both linked to a deepening of JJAS surface pressure conditions over the Arabian Sea. In the first part of the study, we analyze the mean climate response to dust radiative forcing over the domain, discussing notably the relative role of Arabian vs. Indo-Pakistanese dust regions. In the second part of the study, we show that the model skills in reproducing regional dynamical patterns and southern India precipitation trends are significantly improved only when an increasing dust emission trend is imposed on the basis of observations. We conclude that although interannual climate variability might primarily determine the observed regional pattern of increasing dust activity and precipitation during the 2000-2009 decade, the associated dust radiative forcing might in return induce a critical dynamical feedback contributing to enhancing regional moisture convergence and JJAS precipitations over Southern India.

Introduction.

Indian summer Monsoon rainfall determines to a large extent food production for sub-continental India and has major socio-economic impacts. Simulating monsoon precipitations variability from intra-seasonal to inter-annual time scales is identified as major challenge, especially in the context of climate change and increasing anthropogenic pressures over the Indian subcontinent (Lau, et al., 2008). The complexity of the monsoon system arises from the interactions between physical processes involving atmosphere, land and ocean and operating over a wide range of spatial and temporal scales (Turner, et al., 2012). The role of aerosol as a possible factor modifying these interactions, with consequences on precipitation variability, has been a subject of intense study for the last decade (Lau et al., 2008).

There are basically two mechanisms invoked when discussing the climatic response to direct aerosol forcing over southern Asia. The 'solar dimming effect' (Ramanathan, et al., 2005) proposes that the reduction in surface solar radiation due to absorption and scattering by aerosols, which shows a regional maximum over northern India and Indian ocean, induces a reduction of the north-south surface temperature gradients resulting in a weakening of the Indian summer monsoon. Consistently with this mechanism, the observed summertime drying trend observed over Central Indian region since 1950 has been attributed to increased anthropogenic aerosol emissions through a slowdown of the tropical meridional circulation (Bollasina, et al., 2011). In contrast the "elevated heat pump effect' (Lau, et al., 2006) proposes that radiative heating anomalies due to anthropogenic black carbon (BC) and dust transported over the Himalayan foothill

and Tibetan plateau during the dry season and the pre-monsoon enhance meridional tropospheric temperature gradients resulting in a strengthening and earlier onset of the Indian monsoon rainfall. The elevated heat pump effect has however been questioned by Nigam and Bollasina, 2010. Though apparently antagonistic both these mechanisms might be effective at different stage of the pre-monsoon and monsoon development (Meehl, et al., 2008) outlining the complexity of aerosol climate feedbacks operating on different time scales. In addition it has been outlined that the regional impact of Asian aerosol might be reinforced by non Asian sources through long distance transport and global dynamical adjustments (Bollasina, et al., 2013), (Ganguly, et al., 2012), (Cowan, et al., 2011), (Wang, et al., 2009).

Despite a large focus on anthropogenic aerosol effects justified by the observed intensification of emissions contributing to the "Asian brown cloud" (Ramanathan, et al., 2005), the potential importance of natural, and in particular dust, aerosol has been also recently highlighted (Jin, et al., 2014), (Vinoj, et al., 2014): It is suggested that west Asian dust outbreaks can induce a fast and regional atmospheric response which could explain observed positive correlation between aerosol optical depth (AOD) over west Asia and summer precipitation over India on a weekly time scale. Using global circulation model (GCM) experiments with prescribed sea surface temperature (SST) Vinoj et al. (Vinoj, et al., 2014) attributes the cause of this correlation to the large radiative heating induced by dust radiation absorption over Arabia and the Arabian sea resulting in an intensification of south-westerly moisture convergence towards India. This mechanism involves primarily direct and semi-direct aerosol effects and based on a fast reaction of monsoonal weather systems to dust radiative heating perturbation.

48 The question of characterizing the impact of west Asian dust on Indian monsoon
49 becomes even more relevant if we consider another striking fact which is the observed
50 recent enhancement of Arabian dust activity as measured by satellite and ground based
51 AOD observations during the past decade. Based on Sea-viewing Wide Field of View
52 Sensor (SeaWIFS) satellite observations, a significant June-July-August increasing AOD
53 linear trend o has been determined for the period 1998-2010 for the Arbian region (Hsu,
54 et al., 2012). This regional trend, associated to a regional increase of dust storm activity,
55 is also detected in ground based photometer measurements from the Aerosol Robotic
56 Measurement Network (AERONET) at the Solar village site in Saudi Arabia (Xia, 2011).
57 To our knowledge, the attribution of this regional emission increase to climatic factors
58 and/or land use change is yet to be fully investigated. Ginoux et al., 2012 discuss the
59 possible increasing contribution anthropogenic dust sources relevant to the region, and
60 we also indicate later some possible connections with the evolution low pressure
61 conditions over the Arabian sea and the Indian monsoon system.
62 In this context, the question we wish to primarily address here is: What are the
63 main characteristic of dust radiative forcing regional climatic feedbacks, and to which
64 extent the recent enhancement of dust activity in the Arabian region could affect the
65 Indian monsoon dynamics and precipitations on decadal time scale? As dust emissions
66 might evolve naturally or/and as a result of climate and land use change ((Mahowald,
67 2007), (Mulitza, et al., 2010); Yoshioka et al., 2007) characterizing and quantifying the
68 regional climate implications of observed dust variability is especially relevant for a
69 better understanding of the Indian monsoon system variability and its possible evolution.

Toward this goal, we use a 50 km resolution regional climate model coupled to an aerosol scheme and a slab-ocean model together with diverse observation and reanalysis products. A specific attention is paid to the quality of the simulated Indian monsoon circulation and precipitation fields as well as to the representation of aerosols notably in term of sources, optical depth, radiative forcing and heating rates gradients. In our approach, we believe that the simulation domain size is large enough to capture important regional dynamical feedbacks to the aerosol radiative perturbation. As a caveat we acknowledge that large scale dynamical feedbacks arising from the possible aerosol induced excitation of planetary waves (Rodwell and Jung, 2008) cannot be accounted for using a limited area model. Knowing in which proportion the effective regional climatic response to aerosol forcing is primarily dominated by regional vs. global dynamical adjustments is however a matter of debate (Ramanathan, et al., 2005), (Bollasina, et al., 2011), (Ganguly, et al., 2012) (Cowan, et al., 2011). In section 1 we detail the modeling experiments as well as the different data sets and method use for trend calculation. Section 2 focuses on analyzing observed summer AOD and precipitation trends and interannual correlations over the domain. Dust radiative and climatic impacts and the possible links between Arabian dust trend and southern India precipitation at the decadal scale are then addressed in section 3 and 4.

1 Data and methods

1.1 Regional climate model.

We use the International Center for Thoretical Physics (ICTP) regional climate model RegCM4 (Giorgi, et al., 2012) at 50 km resolution. Runs are performed on the COordinated Regional climate Downscaling Experiment (CORDEX)-India domain over the period 1999-2009 including a 1 year spin up. Boundary conditions are provided by ERA-Interim reanalyzes through a 1000 km buffer zone. The Newtonian relaxation to large scale fields applied in the boundary buffer zone is designed to limit as much as possible wave reflections in the domain (Marbaix et al., 2003). Important physical options we used for this study are the Community Land Model version 3.5 (CLM3.5) (Tawfik, et al., 2011), the University of Washington turbulence scheme (O'Brien, et al., 2012) and the Emanuel convection scheme (Emanuel, 1991) with enabled tracer transport capabilities. The RegCM4 aerosol scheme includes a representation of anthropogenic sulfates, black and organic carbon (Solmon, et al., 2006); (Qian, et al., 2001) as well as sea-salt and dust aerosol. For anthropogenic emissions, we use the Regional Emission inventory in ASia (REAS) (Ohara, et al., 2007), (Nair, et al., 2012) completed by the Atmospheric Chemistry and Climate Model Intercomparison Project (ACCMIP) emissions (Lamarque, et al., 2010) to account for biomass burning emissions and REAS-uncovered regions. For natural particles, sea salt aerosol emissions are calculated on line and are represented by two (sub and super-micronic) different bins (Zakey, et al., 2008). The dust emission scheme (Marticorena, et al., 1995), (Zakey, et al., 2006) includes updates of soil texture distribution following (Menut, et al., 2013) and emission size distribution (Kok, 2011), (Nabat, et al., 2012). Lateral Boundary conditions for aerosols are prescribed from a decadal climatology obtained from global runs performed using CAM-Chem model (J. von Hardenberg, personal communication, 2014). Dusts are represented using 4 bins and are impacting short and long wave radiation transfer as detailed in Supplementary Information (Table S1). All other aerosols impact the RegCM shortwave radiation scheme through pre-calculated optical properties (Solmon, et al., 2006). Only the first indirect effect is accounted for and applied to sulfate aerosol (Giorgi, et al., 2003).

Of particular importance for studying aerosol effects (Miller et al., 2004) ;(Zhao, et al., 2011), we implemented in RegCM4 a "flux corrected" slab ocean parameterization following an approach used in the FMS model (http://www.gfdl.noaa.gov/fms-slab-ocean-model-technical-documentation). This parameterization assumes a 50 m depth ocean mixed layer for which we calculate a prognostic SST through a simple energy budget. The lack of ocean dynamics, diffusion and convection, but also other model surface flux errors are compensated by specifying surface flux adjustments (q-flux adjustments) to the slab temperature tendency equation, notably in order to maintain a realistic SST seasonal cycle compared to observations. To derive the q-flux terms, we perform first a "restoring run" (with no interactive dust aerosol) where the slab prognostic SST are restored to observations, taken here as the Optimum Interpolation Sea Surface Temperature (OISST) (Reynolds, et al., 2002), and considering a 5 day restoring time scale. As the slab mixed layer model is integrated (over the 1999-2009 period in this experiment), the restoring heat fluxes (q-flux) calculated through this procedure are archived and saved in a monthly mean climatology at the end of the restoring run. Once the q-flux climatology is built , the control and experimental "adjusted runs" are performed accounting for q-fluxes (prescribed from the climatology) in the slab ocean temperature equation. Over the domain, seasonal average differences of SST between the q-flux adjusted control experiment and OISST observations varies in the range of -1 to 1 degree, ensuring that prognostic SSTs in the adjusted runs do not diverge much from observations and follow a realistic seasonal cycle. This approach extends previous aerosol regional climate studies based on forced SST over the Indian Monsoon and other domains e.g. (Das, et al., 2014).

145 The control experiment consist in a three ensemble members of adjusted runs with
146 no interactive dust aerosol activated (*nodust*). An ensemble of three adjusted runs is then
147 performed with activation of dust (*dust*). Additionally, a sensitivity test consisting in
148 removing the Indo_Pakistanese regional dust source (*dust_noIP*) is also performed.
149 Finally a three ensemble members experiment is made with imposing an increasing
150 emission trend over Arabia in order to better reproduce observed AOD trends (*dust_ft*).
151 This is done by increasing the saltation flux erodibility factor (Marticorena, et al., 1995)
152 during the run. From year 2004 to 2009 the corresponding increase of erodibility factor is
153 about 30 %..In order to limit the effect of internal variability on our analysis of the
154 aerosol feedbacks, we impose a small random perturbation in boundary conditions to
155 every ensemble members during the run following (O'Brien, et al., 2011). With this
156 technique, we increase the filtering of noise *vs.* statistically significant physical signal
157 while performing differences between the ensemble means of perturbed and control
158 runsexperiments. All results, figures and discussion are based on ensemble means.
159

160 **1.2 Aerosol Optical Depth trend calculation.**

161 JJAS AOD linear trend calculations are first performed using the Sea-viewing
162 Wide Field of View Sensor (SeaWIFS) monthly AOD (550 nm) products at 0.5 degree,
163 and regrided on the 50 km RegCM grid. Algorithms and validity of AOD retrievals from
164 SeaWIFS atmospheric corrections are discussed in (Sayer, et al., 2012)a and (Sayer, et
165 al., 2012)b. Moreover, as argued in (Hsu, et al., 2012), the SeaWIFS AOD product is
166 recognized as a "stable" data set minimizing sensor calibration impact on trend analysis
167 For each model grid column, the SeaWIFS AOD are first deseazonalised applying a 13-

168 term moving average for trend first guess and a stable seasonal filter for removing of the
169 seasonal cycle (Brockwell, et al., 2002). The deseasonalized times series of JJAS 2000-
170 2009 are then extracted and a linear regression is applied on this subset to determine the
171 JJAS linear trend. Statistical significance of the trend is determined using a F-test and we
172 plot only statistically significant pixels with a significant non zero slope (p-value < 0.05).
173 Over our region of interest this treatment shows much consistency with the results of Hsu
174 et al., 2012 (Hsu, et al., 2012). The same method is applied to simulated monthly AOD
175 time series for model –measurement comparison. Over the particular location of Solar
176 Village, the deseasonalized JJAS AOD time series is also calculated from the Aerosol
177 Robotic Network (AERONET) monthly optical depths and considering the average of
178 AOD measured at 440nm and 640 nm.
179 In addition to SeaWIF, we also make use of the Multiangle Imaging Spectro-Radiometer
180 (MISR, (Martonchik, et al., 2004)) retrievals for the validation of mean AOD and further
181 interannual variability analysis.
182
183 **1.3 Precipitation trend calculation.**
184 For the 2000-2009 precipitation trend calculation over southern India (Figure
185 1.b), we use the University of East Anglia Climate Research Unit product (CRU) (Harris,
186 et al., 2014), the Tropical Rainfall Measuring Mission (TRMM 3B42) (Huffman, et al.,
187 1995) product, the University of Delaware product (UDEL) (Matsuura, et al., 2009) and
188 the Precipitation Estimation from Remotely Sensed Information using Artificial Neural
189 Networks (PERSIANN) product (Ashouri, et al., 2014).. For each data set, precipitation
190 monthly time series are first geographically averaged over a continental southern Indian

191 box (5-20 N, 60-80 E). Deseasonalized time series are produced following a similar
192 method than for AOD treatment.. A yearly series of JJAS average precipitation is then
193 produced by averaging the different deseaonalized series from each data sets, and
194 keeping the minimum and maximum values for estimation of the spread between
195 different observation data sets.
196 Additionally for the evaluation of simulated mean JJAS precipitation, we also use the
197 "Asian Precipitation - Highly Resolved Observational Data Integration Towards
198 Evaluation of water resources" (APHRODITE) data set over the 2000-2007 period
199 (Yatagai, et al., 2012).
200

201 ## 2 AOD vs precipitation trends and interannual variability correlations.

202

203 Linear trends of JJAS AOD, calculated from SeaWIFS observations over our domain (cf
204 section 1), are presented on Figure 1 and Figure 3.a . As already reported in (Hsu, et al.,
205 2012), a significant positive trend is found over the Arabian Peninsula region. In addition,
206 a positive AOD trend observed at the AERONET station of solar village (Xia, 2011) is
207 also reported (Figure 1.a). As discussed in Hsu et al., 2012 a decreasing trend in
208 AERONET retrieved angstrom coefficient has been observed at Solar Village, indicating
209 an enhanced contribution of larger particles to AOD over the decade. Together with the
210 fact that AOD trends are due to an amplification of seasonal cycle coincident with dust
211 seasonal maximum, this indicates that the Arabian region AOD positive trends are mainly
212 due to increasing dust emission activity vs. a possible anthropogenic contribution. From
213 the time series in Figure 1.a, we note that the JJAS observed deseasonalized AOD tends

214 to steepen around year 2005. Consequently the 2005-2009 pentad shows sensibly higher
215 averaged AOD relative to the 2000-2004 pentad. For simplifying the following
216 discussion we will refer to these pentads as “NONDUSTY” and “DUSTY”.

217 An increasing trend for precipitation over southern and eastern India is also
218 detected in several data sets as illustrated in (Figure 1.b). In a rather similar way to
219 Arabian AOD, the observed JJAS precipitation in Figure 1.b shows a relative
220 intensification for “DUSTY” relative to “NONDUSTY” pentads. If we plot the mean
221 surface pressure and circulation differences between “DUSTY”” and “NONDUSTY””
222 pentads from ERAI and NCEP2 reanalyzes (Figure 4.a and Figure S3), we observe that
223 both data sets show a cyclonic pattern over the Eastern Arabian sea and India with
224 enhanced southwesterly circulation toward continental India. The associated increase of
225 moisture flow over southern India is a likely reason for enhanced precipitations during
226 “DUSTY” pentad relative to “NONDUSTY” pentad observed in precipitation data sets
227 on Figure 1.b.

228 Furthermore, the cyclonic pattern found in pentad differences depicts a relative
229 increase of the frequency/intensity of low pressure situations over northern Arabian sea
230 for “DUSTY” relative to “NONDUSTY” pentad. Such conditions are favorable to
231 enhanced Shamal wind, (Hamidi, et al., 2013), (Notaro, et al., 2013) and could thus be a
232 likely reason for the observed increase of AOD during the decade. On short time scales, it
233 is also known that individual storms moving in the Arabian sea and the northern bay of
234 Bengal can trigger large dust emission from Arabia and the Indo-Pakistanese - Iran desert
235 regions (Kaskaoutis, et al., 2014), (Ramaswamy, 2014). Based on these observations,
236 both enhanced precipitation over India and Arabian dust AOD increase could be linked to

lower pressure conditions prevailing over the Arabian Sea during DUSTY relative to "NONDUSTY" pentads. Reasons for these conditions are likely a feature of climate decadal variability over the region (Patra et al., 2005) and further analysis is beyond the scope of this study

If the arguments developed above are valid, one should also expect a possible correlation between the inter-annual variability of summer dust AOD and precipitation over southern India. This correlation is not obvious on Figure 1 for in the case of Solar Village AOD. In order to get a more regional picture, we extend our analysis by calculating inter-annual correlations between observed deseasonalised summer AOD (based SeaWIFS and MISR data) and deseasonalized summer precipitation over the previously defined southern India box (based on the PERSIANN data set). We consider the 1999-2010 period for SeaWIFS and 2000-2010 for MISR, excluding pixel with JJAS AOD < 0.2 in the process. Pixels with less than 8 years of valid JJAS observations over the period are excluded of the correlation calculation as well. Evident caution must be taken while interpreting the values of correlation coefficients due to the limited sample size. Nevertheless, on Figure 2.a and b, our analysis reveals clear regional patterns: Over the Indo-Pakistanese source region both MISR and SeaWIFS deseasonalised summer AOD tend to be anti-correlated with southern India deseasonalised precipitations. Inversely, over Arabia, positive correlation coefficients tend to be observed for both MISR and SeaWIFS. This analysis has been repeated using the TRMM precipitation data set with no significantly different results (not shown here). Despite the fact that correlations are not very strong, the homogeneity of regional patterns and their consistency through different observational data sets lead us to think that a relation exists

between the interannual variabilitiy of dust sources activity and Indian precipitation. This relation is in line with the previous argument linking cyclonic activity in Arabian sea, associated with more summer precipitation over India and Pakistan, and enhanced Arabian dust emissions. Contrarily to the Arabian Peninsula, the Indo-Pakistanese region is affected by Indian monsoon rainfall. The anti-correlation obtained over this region could thus possibly be explained by enhanced particle wet deposition and/or inhibiting effect of soil moisture on dust emissions during rainy years.

3 Simulation of dust radiative forcings, trends and associated feedbacks

3.1 Simulation of mean JJAS climate.

In this section we assess the model capacity to simulate the mean observed JJAS monsoon circulation and precipitation over the domain. Comparison of simulated JJAS 850 hpa circulation patterns show an overall consistency with ERA-Interim reanalysis in rm of pattern and intensity as illustrated in Figure 5a,b. The main differences are a moderate underestimation of Easterly circulation in the region of the Somalian Jet, and a tendency for the model to overestimate average wind speed over the Bengal gulf and Indonesia. Model mean JJAS precipitations are evaluated using TRMM, PERSIANN and the high resolution APHRODITE data sets (cf section 1). The variability between observations is illustrated on Figure 6, c,e and g. As in many modeling studies and due to the complexity of convective and dynamics processes, important precipitation overestimation biases are found in region of low precipitation as well as over the North

283 Eastern Himalayas and over the southern Bay of Bengal (Figure 6). Over continental
284 India, the control simulation (*nodust*) tends to produce drier conditions than observed,
285 with a relative bias increasing toward Eastern and Southern India (Figure 6,d,f,h). The
286 model shows better results when compared to the high resolution APHRODITE rain
287 gauge based data set (Figure 6,g-h). Comparison of Figure 6,b and 6, d,f,h shows that
288 radiative effects of dust tends to reduce model biases over continental India southern and
289 northwestern regions (see also Figure S4). Biases are however increased over the western
290 bay of Bengal. Overall the simulated mean circulation and precipitation biases obtained
291 in these simulations are either lower, or comparable with CMIP5 state of the art GCMs
292 and multi model ensemble (Sperber, et al., 2013).
293
294 **3.2 Simulation of aerosol optical depth, radiative forcings and heating rates.**
295
296 The climate response to aerosol via direct and semi direct effect is strongly
297 dependant on radiative forcing gradients as well as the vertical distribution of radiative
298 heating due to aerosol. To evaluate model performance in this regard, the AOD simulated
299 for both anthropogenic and natural aerosol is evaluated using MISRand SeaWIFS
300 products described in section 1 (Figure 7). Simulated AOD in regions dominated by
301 anthropogenic emissions (North Eastern India, China, Indonesia) are reasonably captured
302 despite local underestimations for Indian and Chinese megacities. An underestimation of
303 simulated AOD over the Bay of Bengal is however noted, which can be due to
304 uncertainties in emissions, notably for biomass burning (Streets, et al., 2003), and/or an
305 excessive deposition rate due overestimated precipitations as discussed previously.

306 Overall, simulated JJAS 2000-2009 AOD shows a very good agreement with
307 observations both in term of magnitude and spatial gradients, providing additional
308 regional details when compared to existing GCM simulations e.g. (Vinoj, et al., 2014),
309 (Bollasina, et al., 2011), (Lau, et al., 2006). Of particular importance, the dust dominated
310 regions of Arabian peninsula, the Arabian sea and the Indo-Pakistanese desert regions are
311 quite accurately represented in terms of averaged JJAS AOD, although a likely small
312 contribution of non dust aerosol might play in this comparison..
313
314
315 Additional comparisons of simulated AOD and ground based AERONET
316 retrieved AOD (500 nm) are proposed in Figure 8 for the stations of Solar Village,
317 Meizera, Kuwait Airport and Karachi. Dust aerosol mass is known to be dominant over
318 these stations, except perhaps during winter season over Karachi. For both model and
319 observations, monthly averages are built from daily means and screened for missing days
320 in observations. Figure 8 shows that the model tends in general to slightly underestimate
321 observed AOD. This underestimation is perhaps more pronounced for the Karachi
322 station, as also shown on JJAS average AOD comparisons (Figure 7). The simulation of
323 AOD seasonal cycles shows an overall consistency with observations (Figure 9 a,c).
324 However we note that for certain years AOD spring maxima tend to be underestimated by
325 the model over solar village, while summer peaks tends to be overestimated. This slight
326 shift of the seasonal cycle is also discussed in Shalaby et al., 2015.
327 On Figure 9 b,d we compare simulated aerosol size distribution to size
328 distributions retrieved by AERONET inversions and re-binned to match model dust bins.
329 Due to lack of observational data and given the scope of the study, we restrict this

330 comparison to JJAS 2009. Inter-annual variation of JJAS size distribution might anyway
331 be of secondary order, especially given the possible uncertainties in AERONET
332 inversions (Dubovik et al., 2000). For both Solar Village and Karachi, the model tends to
333 show a consistent relative distribution between size bins compared to observations.
334 However we can note an overestimation of simulated fine and/or medium bins compared
335 to underestimated coarse bin, especially in the case of Karachi (Figure 9.d). One of the
336 possible reasons for this might lie in the emission size distribution (Kok et al., 2011) who
337 tends to be more uncertain with regards to representing coarse particles, as for example
338 discussed in Mahowald et al., 2014. Other reasons could be linked to accuracy in sources
339 geo-location, removal and transport processes. Bearing in mind observational
340 uncertainties, the implication of a simulated dust size distribution shifted towards smaller
341 particles would be to enhance SW scattering vs. SW absorption and LW emission with
342 implications on radiative forcing and feedback discussed further. With possible
343 compensating effects, note that dust refractive indices considered in this study are issued
344 from the OPAC data base (cf supplementary material) which could on the contrary
345 enhance absorption as noticed in Kaufman et al., (2001), Moulin et al.,(2001) and
346 Balkanski et al., (2007).

347 Over dust dominated regions, the net dust surface radiative forcing (Figure 10,a)
348 is dominated by shortwave cooling vs. positive long-wave surface warming as reported
349 on supplementary material (Figure S1). This induces a surface temperature cooling
350 illustrated on Figure 10,e which can reach -2K in sub-regions of Arabia. Over the ocean,
351 a surface cooling is also obtained through the slab ocean response, but tends to be less
352 effective due to larger surface thermal inertia. SST cooling reaches up to -1 C close to

353 Oman Gulf with a decreasing gradient towards India (Figure 10, e). As a result of both
354 dust optical properties and surface albedo, top of atmosphere radiative forcing (TOA) is
355 mostly positive over the high emission region of the Arabian peninsula, and becomes
356 negative above the ocean and continental India. Note that in comparison to Arabian
357 peninsula, the TOA radiative forcing efficiencies (i.e. TOA normalized by AOD reported
358 on Figure 10, d) show less of a warming effect in the Indo-Pakistanese desert regions
359 essentially due to lower surface albedo. Over continental India the TOA radiative forcing
360 efficiencies becomes largely negative due to relatively dark albedo and also due to the
361 fact that long range transported dust from Arabian and Indo-pakistanese sources are finer
362 and more scattering. Uncertainties and regional variability in dust size distribution and
363 optical properties might affect the magnitude and even the sign of the radiative forcing
364 simulated here with potential consequence on regional climate feedbacks as discussed
365 further.

366 Atmospheric radiative heating rate anomalies primarily associated to dust
367 radiative absorption, are presented on Figure 10,f and Figure S2. Mean simulated values
368 for JJAS ranges from more than 1 K/Day over source regions of Arabia to about 0.3
369 K/day in the core of the Arabian dust outflow, located between 850 and 600 hpa. Over
370 India, the JJAS dust radiative warming at 850 hp reaches about 0.05 to 0.1 K/day. These
371 values are in the range of different observational studies (Moorthy, et al., 2009),
372 (Kuhlmann, et al., 2010), (Nair, et al., 2008). We note that when radiative and moist
373 processes feedbacks are combined, the diabatic heating induced by dust is however
374 significantly lower than the 2K/day warming reported in (Vinoj, et al., 2014) which can
375 also explain differences further discussed in section 3.

376

377

378 **3.3 Mean monsoon response to dust radiative forcing.**

379

380 Regional climate adjustments to dust radiative forcing are first discussed by
381 comparing '*dust*' and '*nodust*' simulations (as defined in section 1) for JJAS 2000-2009.
382 Figure 11 presents 850 hpa circulation and geopotential height (GPH) anomalies induced
383 by dust direct and semi-direct over the domain. Two patterns emerge from this
384 comparison: The first one is a low GPH anomaly centered over southern Arabian
385 Peninsula associated to a cyclonic circulation, and the second one a positive GPH
386 anomaly roughly centered over North Eastern India associated to an anti-cyclonic
387 anomaly. Regions of large positive or negative values in 850 hpa GPH difference patterns
388 tend to match closely the regional TOA radiative forcing patterns (Figure. 10b). Over
389 Arabia, dust radiative warming is maximum due to high concentration of dust while dust
390 surface cooling efficiency is relatively reduced due to high surface albedo. This induces a
391 deepening of the Arabian thermal low (Figure 11) and dry convection collocated with the
392 maximum of dust radiative warming (Fig S2, c and d). On its southern part, the cyclonic
393 circulation anomaly is associated to an intensification of the Somalia jet and Eastward
394 circulation between 10 and 20 N and 50 to 75 E. This intensification induces an enhanced
395 convergence of moisture flux toward southern India and an increase of convective
396 activity and precipitations over the southern Indian continent (Figure 11 and S2 d, e).
397 From these simulations we estimate that this mechanism could enhance average
398 precipitation by up to 10 % in southern India thus contributing to improve the model dry

399 bias (Figure. 6 a).Up to roughly 20N, our results show much similarity with GCM results
400 notably reported in (Vinoj, et al., 2014). One noticeable difference however is, while
401 (Vinoj, et al., 2014), obtain an increase of precipitation over northern Arabian sea, north
402 western India and Pakistan, convective precipitations tend to be inhibited for these
403 regions in our case. This regional stabilization is induced by a relatively large surface
404 radiative dimming which decreases continental and sea surface temperatures (figure 10
405 ,e), and predominate over dust diabatic e warming effects. This is consistent with a
406 negative simulated TOA radiative forcing (Figure 10 b). Such mechanisms have been
407 analyzed in great details by Miller et al., (2014). On average, in our simulations, the
408 combined contribution of Arabian and Indo Pakistanese dust sources appear to have a
409 dual signature resulting in strengthening the Somalian jet, moisture convergence and
410 precipitation over southern India, while inhibiting convective precipitation and
411 decreasing monsoon intensity north of about 20 N (Figure 11).

412 In order to illustrate further this point, we perform an additional experiment where
413 the Indo-Pakistanese dust sources are removed (*dust_noIP*). By analyzing the difference
414 between *dust_noIP* and *dust* we see that taking into account the Indo-Pakistanese sources
415 results in an inhibition of convergence and precipitation over India (Figure 12). Due to its
416 geographic position and regional surface characteristics, the Indo Pakistanese dust source
417 contributes relatively more than Arabia to the negative TOA radiative forcing and the
418 dimming signal obtained over India. In this regards the Indo-Pakistanese source related
419 effects tends to “compete” with the positive feedback associated to large radiative
420 warming efficiencies over the Arabian Peninsula.

That said, it must be noted that radiative forcings and impacts might strongly depends on dust chemical composition and absorption/scattering properties (Miller et al., 2014; Perlwitz et al., 2001; Solmon, et al., 2008), which exhibit a large regional variability (Deepshikha, et al., 2005), but are unfortunately poorly constrained by observations. In the present simulations we do not account for regional variation of dust refractive indices as proposed in recent studies (Scanza et al., 2015). This point might be especially important over the Indo-Pakistanese region where simulated single scattering albedo might be close to its critical value in relation to surface albedo:. A slight change in optical properties and/or a misrepresentation of size distribution could result in a change in the sign of radiative forcing which can potentially results in an opposite dynamical feedback (in this case an enhancement of elevated heat pump effect over Pakistan and northern India). Some simple tests modifying dust SSA values in RegCM4 and performed over the same domain tend to show that the more absorbing the dust, the more intense is the positive feedback on convergence and precipitation over India (S. Das personal communication, 2015). Finally, note that we do not account for possible dust indirect effects on warm and ice cloud microphysics. There is still a considerable debate in this matter, and impacts are difficult to assess within the scope of the present study.

3.4 Coupling of Arabian dust increasing activity and precipitation variability over the 2000-2009 decade.

Our working hypothesis is that, if the above mechanisms are valid, the observed increasing dust AOD trend over Arabia over the decade 2000-2010 might have been associated with, and perhaps contributing to, a positive impact on circulation and precipitation over southern India. Focusing on model results we see that, although the standard *dust* simulation is able to capture a slightly positive AOD trend over part of the Arabian Peninsula, this trend is nevertheless largely underestimated when compared to observations (Figure 3 a and b). Consistently with the arguments developed before, a likely reason for this underestimation is related to the fact that cyclonic pattern found in reanalyzes pentad difference is also not properly captured by the model as shown in Figure 4.b and c, meaning that the model does not reproduce properly increasing occurrences or/and intensification of Shamal conditions during the decade. These deficiencies are likely to be due to uncertainties in coupled convective and dynamical processes over northern Arabian Sea, Pakistan and Bengal gulf which are extremely challenging to capture properly in climate models (Turner, et al., 2012). In terms of dust AOD, the uncertainties in dust emissions parameterizations could further worsen errors in simulating adequately regional climatic trends (Evan, et al., 2014).

However, since dust trigger a potentially important climatic feedback over the region, it is possible that failure in capturing the increasing Arabian dust trend contributes also to failure in capturing a proper trend in regional climate. To explore this issue, we perform an additional experiment where dust emissions are forced in order to reproduce more realistically the observed JJAS AOD increasing trend (see section 1.2 and Figure 1.a and Figure 3.b and c). This constraint is applied only over the Arabian Peninsula and eventual trend visible over other regions are primarily a results of Arabian dust transport

or simulated spontaneously in response to simulated climate. On the JJAS AOD time series (Figure 1.a) we can note that the adjusted model shows enhanced AOD for "DUSTY" pentad relatively to "NONDUSTY" pentad in a relatively similar way to observations. In term of climatic impact, simulated circulation and surface pressure changes between "NONDUSTY" and "DUSTY" pentads show a rather different behavior whether considering *nodust*, *dust* only, or adjusted *dust_ft* simulations (cf section 1), especially over the Arabian Sea and southern India (Figure 4). With no dust, or when dust increasing emission tendency is not forced, the model tends to reproduce an anti-cyclonic pattern over the Arabian Sea (Figure 4, b and c) and no enhanced westward circulation toward the Indian coast, unlike what is observed in reanalyzes (Figure 4a). When dust tendency is forced however, a westward convergence is obtained between 5 and 20 N, and surface pressure pentad differences over the Arabian sea switch from positive to slightly negative (Figure 8 d). The cyclonic pattern and southward flow clearly seen in reanalyzes is however not well reproduced by the simulation which instead tends to generate a cyclonic pattern shifted to eastern India and Bengal gulf. This indicates that dust radiative trends alone shall not be considered as the main driver for explaining regional circulation changes, and also points out to model limitations. With this in mind, the simulations still tend to show some relatively improved circulation and surface pressure changes when dust are present, and especially when the increasing dust trend is more realistically forced. From these results we suggest that while the cyclonic changes observed between pentad in reanalyzes might be primarily a feature of climate variability, the likely associated increase in JJAS west Asian dust emission and Arabian sea AOD could however determine a possibly important positive feedback contributing to intensify

489 westerly circulation and humidity flux convergence towards the south-western Indian
490 coast. The simulated impact of this feedback on summer precipitation trends over
491 southern India is depicted on Figure 1.b: Simulated JJAS precipitations show an
492 increasing linear trend in *dust_ft* deseasonalized JJAS simulations of about 0.11 mm.day-
493 1.y-1 and close to the value of the JJAS trend calculated from observations (0.13
494 mm.day-1.y-1), when no statistically significant trends are detected in *nodust* and *dust*
495 simulations.
496
497 **4. Conclusion**
498
499 Overall our results emphasize the possible two-way interaction between dust
500 emissions variability and the summer regional climate variability in the Indian monsoon
501 domain for inter-annual to decadal time scale. Using observations and a regional climate
502 model, we suggest that an increasing Arabian dust emission trends could have impacted
503 the Indian monsoon circulation and contributed to explain observed increasing 2000-2009
504 summer precipitations over southern India. There are potentially many global and
505 regional players contributing to monsoon precipitation inter-annual and decadal
506 variability (e.g. Indian Ocean Dipole, ENSO, Patra et al., 2005) and dust radiative forcing
507 shall not be considered as the main driver of the observed precipitation interannual and
508 decadal variability. Dust radiative forcing might however determine a positive dynamical
509 feedback favoring the establishment of lower pressure conditions over the Arabian Sea
510 likely associated with both enhanced Arabian dust emissions and precipitation over

511 southern India. Please note however that the entire feedback loop has not been fully
512 demonstrated here since we used forced emission trends.

513 This study does not consider any trend in anthropogenic aerosol emissions during
514 the decade. Increasing AOD trends attributed to anthropogenic pollution have been
515 measured over continental India, though mostly significant during the winter season
516 (Babu et al.,2013). Nevertheless, it is likely there has been an impact of the
517 anthropogenic aerosol trend on Monsoon rainfall during the studied decade, as for
518 example discussed in Bollasina et al., 2011 (who conclude in general to a drying effect of
519 anthropogenic aerosol on continental India). Note that in magnitude, the measured dust
520 decadal AOD trends over Arabia and the Arabian Sea are equally if not more important
521 than AOD trends attributed to pollution increase over India (Babu, et al., 2013)

522 In view of these results, capturing the positive feedbacks between dynamics and
523 dust emission trends in climate models could lead to a more realistic representation of
524 precipitation decadal variability over India. This is even more relevant when considering
525 the emergence and potential importance of “anthropogenic dust sources” as discussed in
526 Ginoux et al., 2012. However, the present study, as well as (Evan, et al., 2014), show that
527 current dust parameterizations and implementations in climate and Earth System models
528 have difficulties to reproduce observed regional AOD inter-annual and decadal
529 variability. Improvement of models whether they deal with dust emissions processes,
530 regional land use change and surface wind speed downscaling are still of primary
531 importance.

532

533

Acknowledgement.

The authors would like to thank two anonymous reviewers for their very useful comments, Jost von Hardenberg for providing aerosol large scale fields for boundary conditions, R. Farneti and F. Kucharski for advices on slab ocean implementation and scientific discussion as well as G. Giuliani and the RegCM developing team for maintaining and managing the code. The authors would also like to thanks all the research teams involved in the creation and maintenance of aerosol and precipitation observational products used in this study.

Ashouri, H., Hsu, K.--L., Sorooshian, S., Braithwaite, D. K., Knapp, K. R., Cecil, L. D., and Prat, O. P.: PERSIANN--CDR: Daily Precipitation Climate Data Record from Multi--Satellite Observations for Hydrological and Climate Studies. Bull. Amer. Meteor. Soc, doi: 10.1175/BAMS-D-13-00068.1, 2014.

Babu, S. S., Manoj, M., Moorthy, K. K., Gogoi, M. M., Nair, V. S., Kompalli, S. K., Satheesh, S.K., Niranjan, K.,Ramagopal, K., Bhuyan P.K. and Darshan Singh: Trends in aerosol optical depth over Indian region: Potential causes and impact indicators. J. Geophys. Res., 118(D20), 11794--11806, 2013.

Balkanski, Y., Schulz, M., Claquin, T., and Guibert, S.: Reevaluation of Mineral aerosol radiative forcings suggests a better agreement with satellite and AERONET data, Atmos. Chem. Phys., 7, 81-95, doi:10.5194/acp-7-81-2007, 2007.

Bollasina, M. A., Ming, Y., and Ramaswamy, V.: Anthropogenic aerosols and the weakening of the South Asian summer monsoon. Science, 334(6055), 502--505, 2011

Bollasina, M. A., Ming, Y., and Ramaswamy, V.: Earlier onset of the Indian monsoon in the late twentieth century: The role of anthropogenic aerosols. Geophys. Res. Lett., 40(14), 3715--3720, 2013.

Brockwell, P. J., and Davis, R. A.: Introduction to time series and forecasting (Vol. 1). Taylor and Francis, 2002.

Cowan, T., and Cai, W.: The impact of Asian and non--Asian anthropogenic aerosols on 20th century Asian summer monsoon. Geophys. Res. Lett., 38(11), doi:10.1029/2011GL047268, 2011.

Das, S., Dey, S., and Dash, S.: Impacts of aerosols on dynamics of Indian summer monsoon using a regional climate model. Climate Dyn., 1--13, 2014.

Deepshikha, S., Satheesh, S., and Srinivasan, J.: Regional distribution of absorbing efficiency of dust aerosols over India and adjacent continents inferred using satellite remote sensing. Geophys. Res. Lett., 32, L03811----L03811, 2005.

Dubovik, O. and King, M. D.: A flexible inversion algorithm for retrieval of aerosol optical properties from Sun and sky radiance measurements, J. Geophys. Res., 105, 20673–20696, 2000.

Emanuel, K. A.: A scheme for representing cumulus convection in large--scale models. J. Atmos. Sci., 48(21), 2313--2329, 1991.

Evan, A. T., Flamant, C., Fiedler, S., and Doherty, O.: An analysis of aeolian dust in climate models. Geophys. Res. Lett., 41(16), 5996--6001, 2014.

Ganguly, D., Rasch, P. J., Wang, H., and Yoon, J.--H.: Climate response of the South Asian monsoon system to anthropogenic aerosols. J. Geophys. Res., 117(D13), doi:10.1029/2012JD017508 , 2012.

Ginoux, P., Prospero, J.M., Gill, T.E., Hsu, N.C. and Zhao M., , Global-scale attribution of anthropogenic and natural dust sources and their emission rates based on MODIS Deep Blue aerosol products, Rev. Geophys., 50, RG3005, doi:10.1029/2012RG000388, 2012.

Giorgi, F., Bi, X., and Qian, Y.: Indirect vs. direct effects of anthropogenic sulfate on the climate of East Asia as simulated with a regional coupled climate--chemistry/aerosol model. Climatic Change, 58(3), 345--376, 2003.

Giorgi, F., Coppola, E., Solmon, F., Mariotti, L., Sylla, M., Bi, X., and others: RegCM4: model description and preliminary tests over multiple CORDEX domains. Climate Research, 52(1), 7--29, 2012.
Hamidi, M., Kavianpour, M. R., and Shao, Y.: Synoptic analysis of dust storms in the Middle East. Asia--Pacific Journal of Atmospheric Sciences, 49(3), 279--286, 2013.
Harris, I., Jones, P., Osborn, T., and Lister, D.: Updated high--resolution grids of monthly climatic observations----the CRU TS3. 10 Dataset. International Journal of Climatology, 34(3), 623--642, 2014.
Hsu, N. C., Gautam, R., Sayer, A. M., Bettenhausen, C., Li, C., Jeong, M. J., and Holben, B. N.: Global and regional trends of aerosol optical depth over land and ocean using SeaWiFS measurements from 1997 to 2010. Atmos. Chem. Phys., 12(17), 8037--8053, 2012.
Huffman, G. J., Adler, R. F., Rudolf, B., Schneider, U., and Keehn, P. R.: Global precipitation estimates based on a technique for combining satellite--based estimates, rain gauge analysis, and NWP model precipitation information. J. Climate, 8(5), 1284--1295, 1995.
Jin, Q., Wei, J., and Yang, Z.-L.: Positive response of Indian summer rainfall to Middle East dust. Geophys. Res. Lett., 41(11), 4068--4074, 2014.
Kaufman, Y. J., Tanr´e, D., Dubovik, D. O., Karnieli, A., and Remer,L. A.: Absorption of sunlight by dust as inferred from satellite and ground-based remote sensing, Geophys. Res. Lett., 28, 1479–1482, 2001.
Kaskaoutis, D., Rashki, A., Houssos, E., Goto, D., and Nastos, P.: Extremely high aerosol loading over Arabian Sea during June 2008: The specific role of the atmospheric dynamics and Sistan dust storms. Atmos. Environ., 94, 374--384, 2014.
Kok, J. F.: A scaling theory for the size distribution of emitted dust aerosols suggests climate models underestimate the size of the global dust cycle. Proc. Natl. Acad. Sci. U. S. A., 108(3), 1016--1021, 2011.
Kuhlmann, J., and Quaas, J.: How can aerosols affect the Asian summer monsoon? Assessment during three consecutive pre-monsoon seasons from CALIPSO satellite data. Atmos. Chem. Phys., 10(10), 4673--4688, 2010.
Lamarque, J.--F., Bond, T. C., Eyring, V., Granier, C., Heil, A., Klimont, Z., and others.: Historical (1850--2000) gridded anthropogenic and biomass burning emissions of reactive gases and aerosols: methodology and application. Atmos. Chem. Phys., 10(15), 7017--7039, 2010.
Lau, K., Kim, M., and Kim, K.: Asian summer monsoon anomalies induced by aerosol direct forcing: the role of the Tibetan Plateau. Climate Dyn., 26(7-8), 855--864, 2006.
Lau, K., Tsay, S., Hsu, C., Chin, M., Ramanathan, V., Wu, G., and others.: The Joint Aerosol--Monsoon Experiment: A new challenge for monsoon climate research. Bull. Amer. Meteor. Soc., 89(3), 369--383, 2008.
Mahowald, N. M.: Anthropocene changes in desert area: Sensitivity to climate model predictions. Geophys. Res. Lett., 34(18), doi:10.1029/2007GL030472, 2007.
Marbaix, P., Gallee, H., Brasseu, O., and van Ypersele, J,-P: Lateral Boundary Conditions in Regional Climate Models: A Detailed Study of the Relaxation Procedure, Mon. Wea. Rev.,131, 461-479, 2003.
Marticorena, B., and Bergametti, G.: Modeling the atmospheric dust cycle: 1. Design of a soil--derived dust emission scheme. J. Geophys. Res., 100(D8), 16415--16430, 1995.

Martonchik, J. V., Diner, D. J., Kahn, R., Gaitley, B., and Holben, B. N.: Comparison of MISR and AERONET aerosol optical depths over desert sites. Geophys. Res. Lett., 31(16), doi:10.1029/2004GL019807, 2004.

Matsuura, K., and Willmott, C. J.: Terrestrial precipitation: 1900-2008 gridded monthly time series, Department of Geography Center for Climatic Research, University of Delaware, 2009.

Meehl, G. A., Arblaster, J. M., and Collins, W. D.: Effects of black carbon aerosols on the Indian monsoon. J. Climate, 21(12), 2869--2882, 2008.

Menut, L., Perez, C., Haustein, K., Bessagnet, B., Prigent, C., and Alfaro, S.: Impact of surface roughness and soil texture on mineral dust emission fluxes modeling. J. Geophys. Res., 118(12), 6505--6520, 2013.

Miller, R.L., Perlwitz, J.P. and Tegen, I.: Modeling Arabian dust mobilization during the Asian summer monsoon: The effect of prescribed versus calculated SST. Geophys. Res. Lett., 30, L22214, doi:10.1029/2004GL020669, 2004.

Miller, R.L., P. Knippertz, C. Pérez García-Pando, J.P. Perlwitz, and I. Tegen, (2014) Impact of dust radiative forcing upon climate. In Mineral Dust: A Key Player in the Earth System. P. Knippertz, and J.-B.W. Stuut, Eds. Springer, 327-357, doi:10.1007/978-94-017-8978-3_13, 2014.

Moorthy, K. K., Nair, V. S., Babu, S. S., and Satheesh, S.: Spatial and vertical heterogeneities in aerosol properties over oceanic regions around India: Implications for radiative forcing. Quart. J. Roy. Meteor. Soc., 135(645), 2131--2145, 2009.

Moulin, C., Gordon, H. R., Banzon, V. F., and Evans, R. H.: Assessment of Saharan dust absorption in the visible from Sea-WiFS imagery, J. Geophys. Res., 106(D16), 18 239–18 250, doi:10.1029/2000JD900812, 2001.

Mulitza, S., Heslop, D., Pittauerova, D., Fischer, H. W., Meyer, I., Stuut, J.--B., and others.: Increase in African dust flux at the onset of commercial agriculture in the Sahel region. Nature, 466(7303), 226--228, 2010.

Nabat, P., Solmon, F., Mallet, M., Kok, J., and Somot, S.: Dust emission size distribution impact on aerosol budget and radiative forcing over the Mediterranean region: a regional climate model approach. Atmos. Chem. Phys., 12(21), 10545--10567, 2012.

Nair, V. S., Babu, S. S., and Moorthy, K. K.: Aerosol characteristics in the marine atmospheric boundary layer over the Bay of Bengal and Arabian Sea during ICARB: Spatial distribution and latitudinal and longitudinal gradients. J. Geophys. Res., 113(D15), doi:10.1029/2008JD009823, 2008.

Nair, V. S., Solmon, F., Giorgi, F., Mariotti, L., Babu, S. S., and Moorthy, K. K.: Simulation of South Asian aerosols for regional climate studies. J. Geophys. Res., 117(D4), doi:10.1029/2011JD016711, 2012.

Nigam, S., and Bollasina M., "Elevated heat pump" hypothesis for the aerosol monsoon hydroclimate link: "Grounded" in observations?: J. Geophys. Res., 115, D16201, doi:10.1029/2009JD013800, 2010.

Notaro, M., Alkolibi, F., Fadda, E., and Bakhrjy, F.: Trajectory analysis of Saudi Arabian dust storms. J. Geophys. Res., 118(12), 6028--6043, 2013.

O'Brien, T. A., Sloan, L. C., and Snyder, M. A.: Can ensembles of regional climate model simulations improve results from sensitivity studies? Climate Dyn., 37(5--6), 1111--1118, 2011.

O'Brien, T., Chuang, P., Sloan, L., Faloona, I., and Rossiter, D.: Coupling a new turbulence parametrization to RegCM adds realistic stratocumulus clouds. Geoscientific Model Development, 5(4), 989--1008, 2012.

Ohara, T., Akimoto, H., Kurokawa, J.--i., Horii, N., Yamaji, K., Yan, X., and Hayasaka, T.: An Asian emission inventory of anthropogenic emission sources for the period 1980-2020. Atmos. Chem. Phys., 7(16), 4419--4444, 2007.

Patra, P. K., Behera, S. K., Herman, J. R., Maksyutov, S., Akimoto, H., and Yamagata, Y.: The Indian summer monsoon rainfall: interplay of coupled dynamics, radiation and cloud microphysics, Atmos. Chem. Phys., 5, 2181-2188, doi:10.5194/acp-5-2181-2005, 2005.

Perlwitz, J.P., Tegen, I. and Miller,R.L.: Interactive soil dust aerosol model in the GISS GCM: 1. Sensitivity of the soil dust cycle to radiative properties of soil dust aerosols. J. Geophys. Res., 106, 18167--18192, doi:10.1029/2000JD900668.

Qian, Y., Giorgi, F., Huang, Y., Chameides, W., and Luo, C.: Regional simulation of anthropogenic sulfur over East Asia and its sensitivity to model parameters. Tellus B, 53(2), 171--191, 2001 .

Ramanathan, V., Chung, C., Kim, D., Bettge, T., Buja, L., Kiehl, J., Washington W.M., Fu Q., Sikka D.R. and Wild, M.: Atmospheric brown clouds: Impacts on South Asian climate and hydrological cycle. Proc. Natl. Acad. Sci. U. S. A., 102(15), 5326--5333, 2005.

Ramaswamy, V.: Influence of Tropical Storms in the Northern Indian Ocean on Dust Entrainment and Long--Range Transport. In Typhoon Impact and Crisis Management (pp. 149--174). Springer, 2014.

Reynolds, R. W., Rayner, N. A., Smith, T. M., Stokes, D. C., and Wang, W.: An improved in situ and satellite SST analysis for climate. J. Climate, 15(13), 1609--1625, 2002.

Rodwell, M. J. and Jung, T.: Understanding the local and global impacts of model physics changes: An aerosol example, Q. J. R. Meteorol. Soc., V134(635), 1479–1497, doi:10.1002/qj.298, 2008.

Sayer, A. M., Hsu, N. C., Bettenhausen, C., Ahmad, Z., Holben, B. N., Smirnov, A., . . . Zhang, J.: SeaWiFS Ocean Aerosol Retrieval (SOAR): Algorithm, validation, and comparison with other data sets. J. Geophys. Res., 117(D3), doi:10.1029/2011JD016599, 2012.

Sayer, A., Hsu, N., Bettenhausen, C., Jeong, M.--J., Holben, B., and Zhang, J.: Global and regional evaluation of over--land spectral aerosol optical depth retrievals from SeaWiFS. Atmospheric Measurement Techniques, 5(7), 1761--1778, 2012.

Scanza, R. A., Mahowald, N., Ghan, S., Zender, C. S., Kok, J. F., Liu, X., Zhang, Y., and Albani, S.: Modeling dust as component minerals in the Community Atmosphere Model: development of framework and impact on radiative forcing, Atmos. Chem. Phys., 15, 537-561, doi:10.5194/acp-15-537-2015, 2015.

Shalaby, A., B. Rappenglueck, E. A. B. Eltahir, the climatology over the arabian peninsula, atmos. chem. phys. discuss., 15, 1523-1571, 2015 doi:10.5194/acpd-15-1523-2015

Solmon, F., Giorgi, F., and Liousse, C.: Aerosol modelling for regional climate studies: application to anthropogenic particles and evaluation over a European/African domain. Tellus B, 58(1), 51--72, 2006.

Solmon, F., Mallet, M., Elguindi, N., Giorgi, F., Zakey, A., and Konaré, A.: Dust aerosol impact on regional precipitation over western Africa, mechanisms and sensitivity to absorption properties. Geophys. Res. Lett., 35(24), doi:10.1029/2008GL035900, 2008.

Sperber, K. R., Annamalai, H., Kang, I.-S., Kitoh, A., Moise, A., Turner, A., and Zhou, T.: The Asian summer monsoon: an intercomparison of CMIP5 vs. CMIP3 simulations of the late 20th century. Climate Dyn., 41(9--10), 2711--2744, .2013.

Streets, D. G., Bond, T. C., Carmichael, G. R., Fernandes, S. D., Fu, Q., He, D., and Yarber, K. F.: An inventory of gaseous and primary aerosol emissions in Asia in the year 2000. J. Geophys. Res., 108(D21), doi:10.1029/2002JD003093, 2003.

Tawfik, A. B., and Steiner, A. L.: The role of soil ice in land--atmosphere coupling over the United States: A soil moisture–precipitation winter feedback mechanism. J. Geophys. Res., 116(D2), doi:10.1029/2010JD014333, 2011.

Turner, A. G., and Annamalai, H.: Climate change and the South Asian summer monsoon. Nature Climate Change, 2(8), 587--595, 2012.

Vinoj, V., Rasch, P. J., Wang, H., Yoon, J.-H., Ma, P.-L., Landu, K., and Singh, B.: Short-term modulation of Indian summer monsoon rainfall by West Asian dust. Nature Geoscience, 7, 308--313, 2014. .

Wang, C., Kim, D., Ekman, A. M., Barth, M. C., and Rasch, P. J.: Impact of anthropogenic aerosols on Indian summer monsoon. Geophys. Res. Lett., 36(21), doi:10.1029/2009GL040114, 2009.

Xia, X.: Variability of aerosol optical depth and Angstrom wavelength exponent derived from AERONET observations in recent decades. Environ. Res. Lett., 6(4), 44011--44019, 2011.

Yatagai, A., Kamiguchi, K., Arakawa, O., Hamada, A., Yasutomi, N., and Kitoh, A.: APHRODITE: Constructing a long--term daily gridded precipitation dataset for Asia based on a dense network of rain gauges. Bull. Amer. Meteor. Soc., 93(9), 1401--1415, 2012.

Yoshioka, M., Mahowald, N., Conley, A., Collins, W., Fillmore, D., and Coleman, D.: Impact of desert dust radiative forcing on Sahel precipitation: relative importance of dust compared to sea surface temperature variations, vegetation changes and greenhouse gas warming, J. Climate, 20, 1445–1467, 2007

Zakey, A. S., Giorgi, F., and Bi, X.: Modeling of sea salt in a regional climate model: Fluxes and radiative forcing. J. Geophys. Res., 113(D14), doi:10.1029/2007JD009209, 2008.

Zakey, A., Solmon, F., and Giorgi, F.: Implementation and testing of a desert dust module in a regional climate model. Atmospheric Chemistry and Physics, 6(12), 4687--4704, 2006.

Zhao, C., Liu, X., Ruby Leung, L., and Hagos, S.: Radiative impact of mineral dust on monsoon precipitation variability over West Africa. Atmos. Chem. Phys., 11(5), 1879--1893, 2011. .

Figure Legends.

Figure 1. Arabian AOD and Southern India deseasonalized precipitation trends during the decade 2000-2009. **(a)** The thick blue line represents monthly deseasonalised time series of JJAS AOD obtained from the Solar Village AERONET station (monthly product, average of 480-640 nm spectral bands). A quadratic regression fit, showing the progressive intensification of observed dust activity is superimposed (blue curve). The blue hatched line represents the deasesonalised AOD time series obtained from SeaWIFS AOD interpolated on the Solar Village station. The green lines represents the monthly deseasonalized time series (as well as the corresponding quadratic fit) of JJAS AOD simulated by the model in *dust* simulation. The red lines represents the monthly deseasonalized time series (as well as the corresponding quadratic fit) of JJAS AOD simulated by the model with forced dust emission trends (*dust_ft* simulation). **(b)** The blue line represents the yearly time evolution of observed continental precipitation averaged for JJAS, over a southern India box (5-20N; 60-80E) and for different data sets (TRMM, CRU, PERSIANN). The blue bars materialize the amplitude between maximum and minimum values amongst observations for a given year. The equivalent deseasonalized JJAS average simulated precipitations are reported for the *nodust* simulations (black line), the *dust* standard simulations (green line) and the forced emission trend *dust_ft* simulations (red line). All modeling results represent a 3 member's ensemble mean.

Figure2. Interannual variability correlation coefficients calculated between deseasonalised summer (JJAS) AOD and deseasonalised JJAS precipitations averaged over a southern India box(5-20N; 60-80E). (a) based on the SeaWIFS AOD retrieval over the 1999-2010 period.(b) based on MISR AOD retrieval over the 2000-2010 period. Pixel showing monthly AOD < 0.2 are excluded from the calculation as well as pixel for which sampled valid year number is less than 8.

Figure 3. Linear JJAS AOD trend calculated over the 2000-2009 period from: (a) SeaWIFS monthly observations, (b) Model standard *dust* simulations, and (d) Model *dust_ft* simulations including a forced emission trend over the Arabian Peninsula. Only statistically significant trends (p-value < 0.05) are represented (cf Data and Methods). All modeling results represent a 3 member's ensemble mean.

Figure 4. Difference of mean JJAS 850 hpa circulation and surface pressure between "DUSTY" (2005-2009) and "NONDUSTY" (2000-2004) pentads as defined in the text and calculated from : (a) ERAI reanalysis, (b) '*nodust*' simulations, (c) '*dust*' standard simulations, (d) '*dust_ft*' simulations with forced emission trend over Arabia. As a complement to ERAI, an equivalent graph has been produced from NCEP reanalyzes and displayed in Figure SI. All simulated results represent a 3 members ensemble mean.

Figure 5. Mean 850 hpa JJAS wind intensity and direction as seen in (a) the ERAI reanalysis and (b) the RegCM *nodust* simulation for the period 2000-2009 and over the CORDEX-India domain. All modeling results represent a 3 member's ensemble mean.

Figure 6. (a) Mean JJAS 2000-2009 precipitation simulated by the model in "*nodust*" configurations. (b) Relative difference in precipitation between *dust* and *nodust* simulations for JJAS 2000-2009 and calculated as *(dust –nodust / nodust) X 100*. (c) JJAS 2000-2009 TRMM precipitation. (d) Relative difference (bias) between *nodust* and TRMM precipitations for observed precipitation level > 0.2 mm/day. (e-f) Same than (c-d) for the PERSIANN data set. (g-h) Same than (c-d) for the APHRODITE data sets, but calculated for JJAS 2000-2007 only. All modeling results represent a 3 member's ensemble mean.

Figure 7. JJAS 2000-2009 AOD seen from the (a) MISR sensor and (b) as simulated by RegCM "*dust*" simulation for the full CORDEX-India domain. JJAS composite averages are built form monthly observations and model outputs. Regions of missing observations are screened out from the model averages. (c, d) Same as (a, b) but using the SeaWIFS AOD observations. All modeling results represent a 3 member's ensemble mean.

Figure 8. Simulated monthly AOD vs AERONET measured monthly AOD for the period of 2000-2009. Blue dots represents the solar Village Station (46.40E, 24.90N), red dot represents the Karachi station (67.03E, 24.87N), green dots represents Kuwait Airport station (47.98E, 29.22N) and black dots the Meizera station (53.8E, 23.15N). The correlation coefficient between data and measurements is equal to 0.59 and the root mean square error is 0.16.

Figure 9. (a) Comparison between simulated and AERONET monthly AOD (see text) for Solar Village station. (b) Comparison of simulated and measured aerosol normalized volume size distribution averaged for JJAS 2009 over Solar Village. For comparison, the AERONET normalized volume distribution (green dotted line) is re-binned using a weighted average between model bins cut-off diameters (red lines). Blue lines show the corresponding simulated 4 bin distribution for the same cut-off diameters. (c) Same than (a) for Karachi station. (d) Same than (b) for Karachi station.

Figure 10. (a) JJAS 2000-2009 Dust aerosol surface radiative forcing diagnostic. (b) JJAS 2000-2009 Dust top of atmosphere radiative forcing diagnostic. (c) and (d) Corresponding surface radiative forcing efficiencies.(e) JJAS 2000-2009 2 m temperature difference between *dust* and *nodust* simulations. (f) 850 hpa radiative heating rate difference between *dust* and *nodust* simulations. All modeling results represent a 3 member's ensemble mean.

Figure 11. Dust impact on the mean monsoon dynamic and precipitations over the period JJAS 2000-2009. (a) 850 hpa geopotential heights (GPH) and monsoon circulation dust induced anomalies calculated as the GPH difference between *dust* and *nodust* simulations. (b) Dust induced precipitation anomaly. The dotted region defines statistically significant results at the 95 % confidence level. All modeling results represent a 3 member's ensemble mean.

Figure 12. Impact of the Indo-Pakistanese dust source compared to the dust simulation calculated as *dust_noIP* - *dust* over the period JJAS 2000-2009. (a) 850 hpa geopotential heights (GPH) and circulation change. (b) Precipitation changes. The dotted region defines statistically significant results at the 95 % confidence level. All modeling results represent a 3 member's ensemble mean.

Figures.

Figure 1.

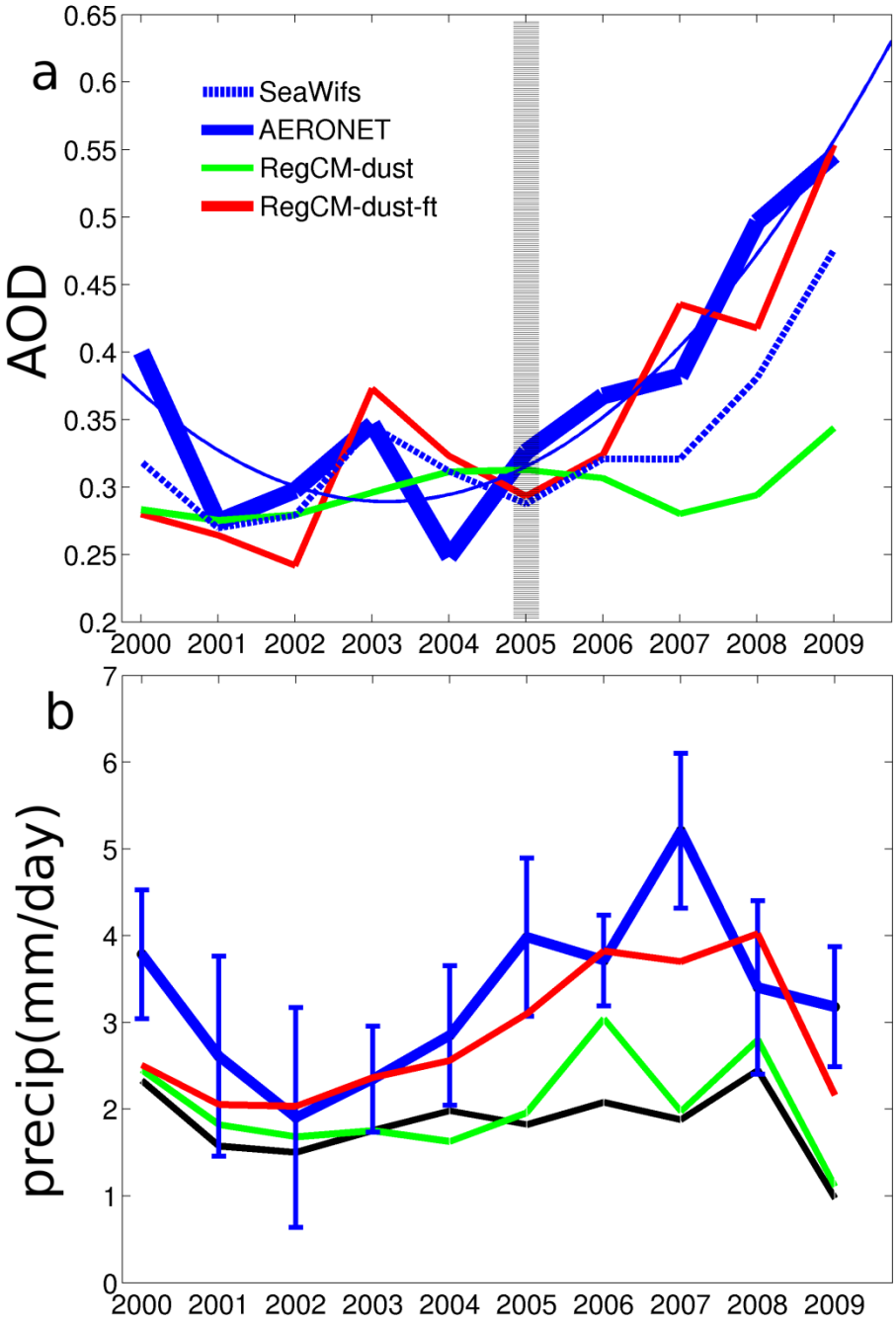

Figure 2.

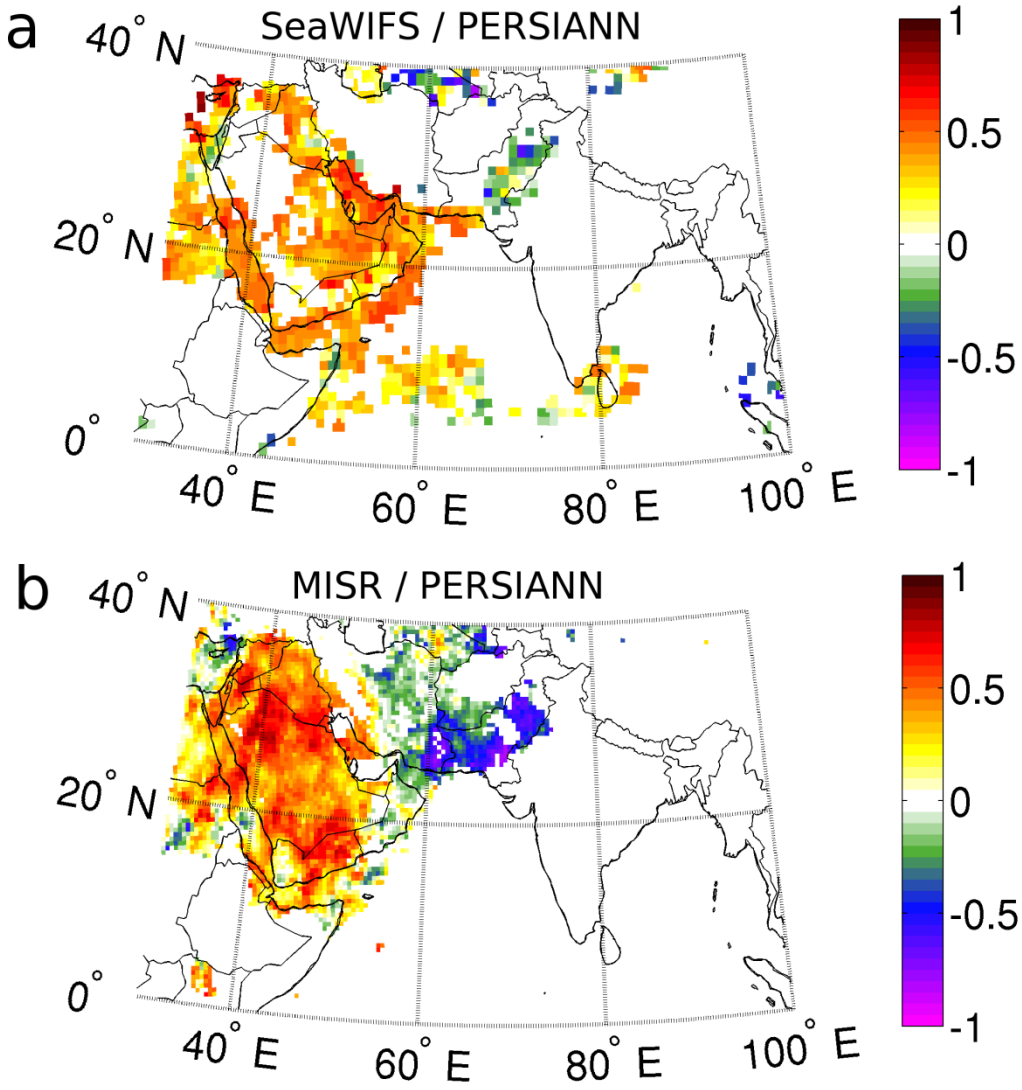
a
SeaWIFS / PERSIANN
40° N
20° N
0°
40° E
60° E
80° E
100° E
1
0.5
0
-0.5
-1
b
MISR / PERSIANN
40° N
20° N
0°
40° E
60° E
80° E
100° E
1
0.5
0
-0.5
-1

Figure 3.

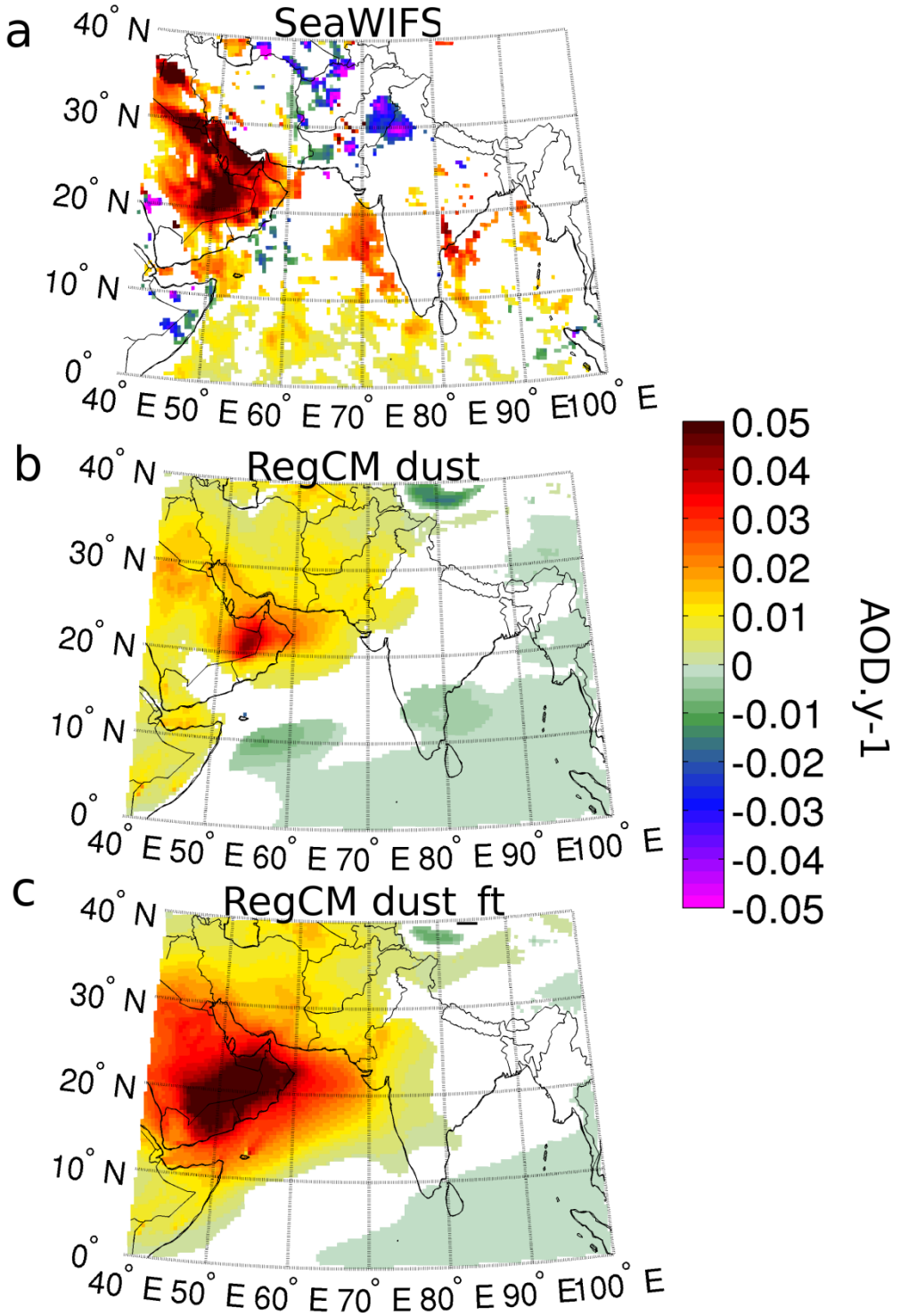
a
SeaWIFS
b
RegCM dust
c
RegCM dust_ft
40° N
30° N
20° N
10° N
0°
40° E 50° E 60° E 70° E 80° E 90° E100° E
0.05
0.04
0.03
0.02
0.01
0
-0.01
-0.02
-0.03
-0.04
-0.05
AOD.y-1

Figure 4.

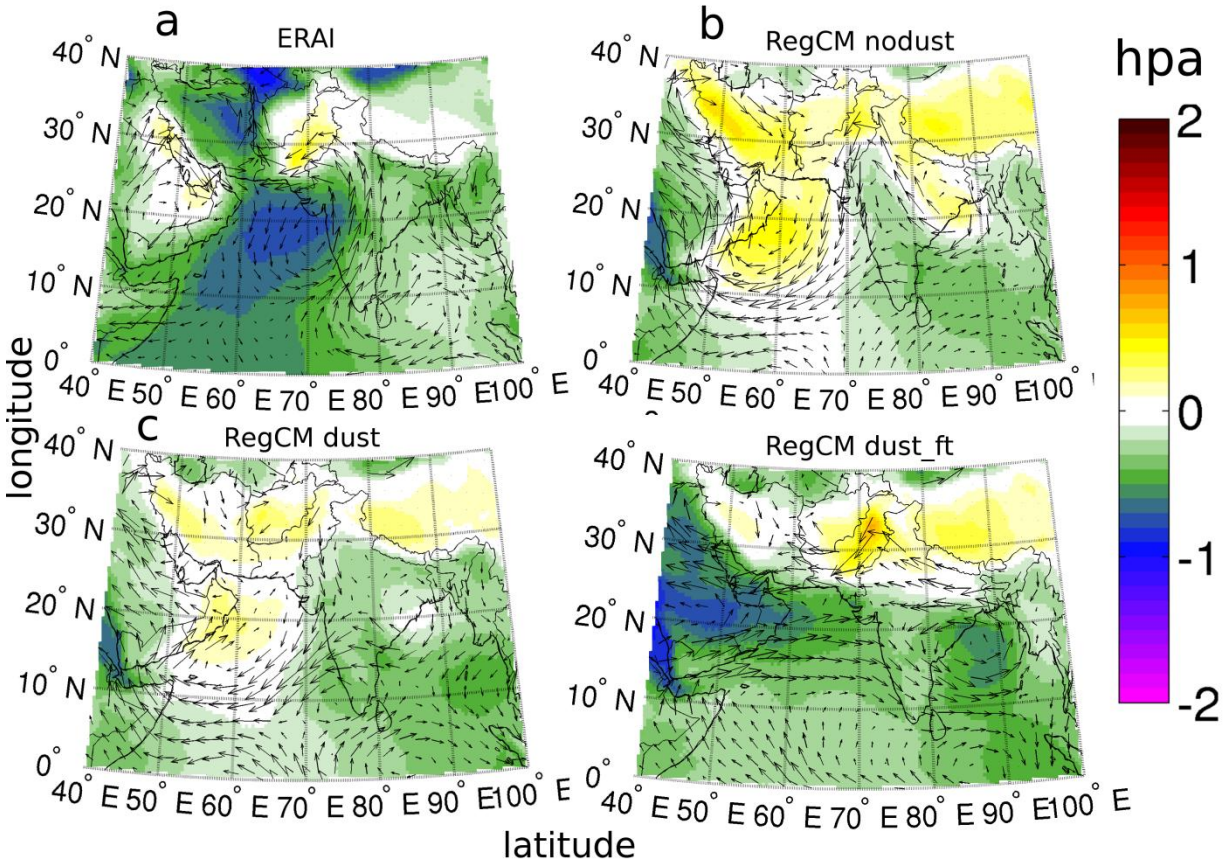
a
ERAI
b
RegCM nodust
c
RegCM dust
RegCM dust_ft
hpa
2
1
0
-1
-2
longitude
latitude
40° N
30° N
20° N
10° N
0°
40° E 50° E 60° E 70° E 80° E 90° E 100° E

Figure 5.

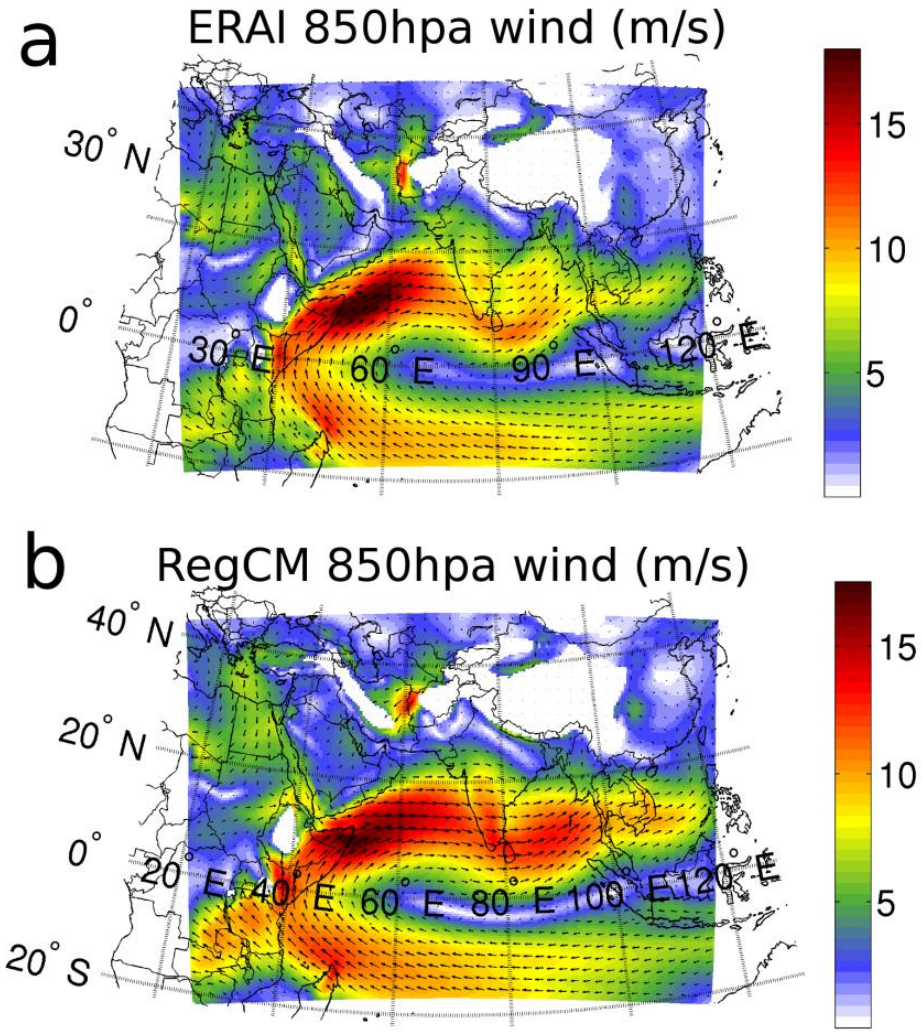
a
ERAI 850hpa wind (m/s)
30° N
0°
30° E
60° E
90° E
120° E
15
10
5
b
RegCM 850hpa wind (m/s)
40° N
20° N
0°
20° S
20° E
40° E
60° E
80° E
100° E
120° E
15
10
5

5

Figure 6.

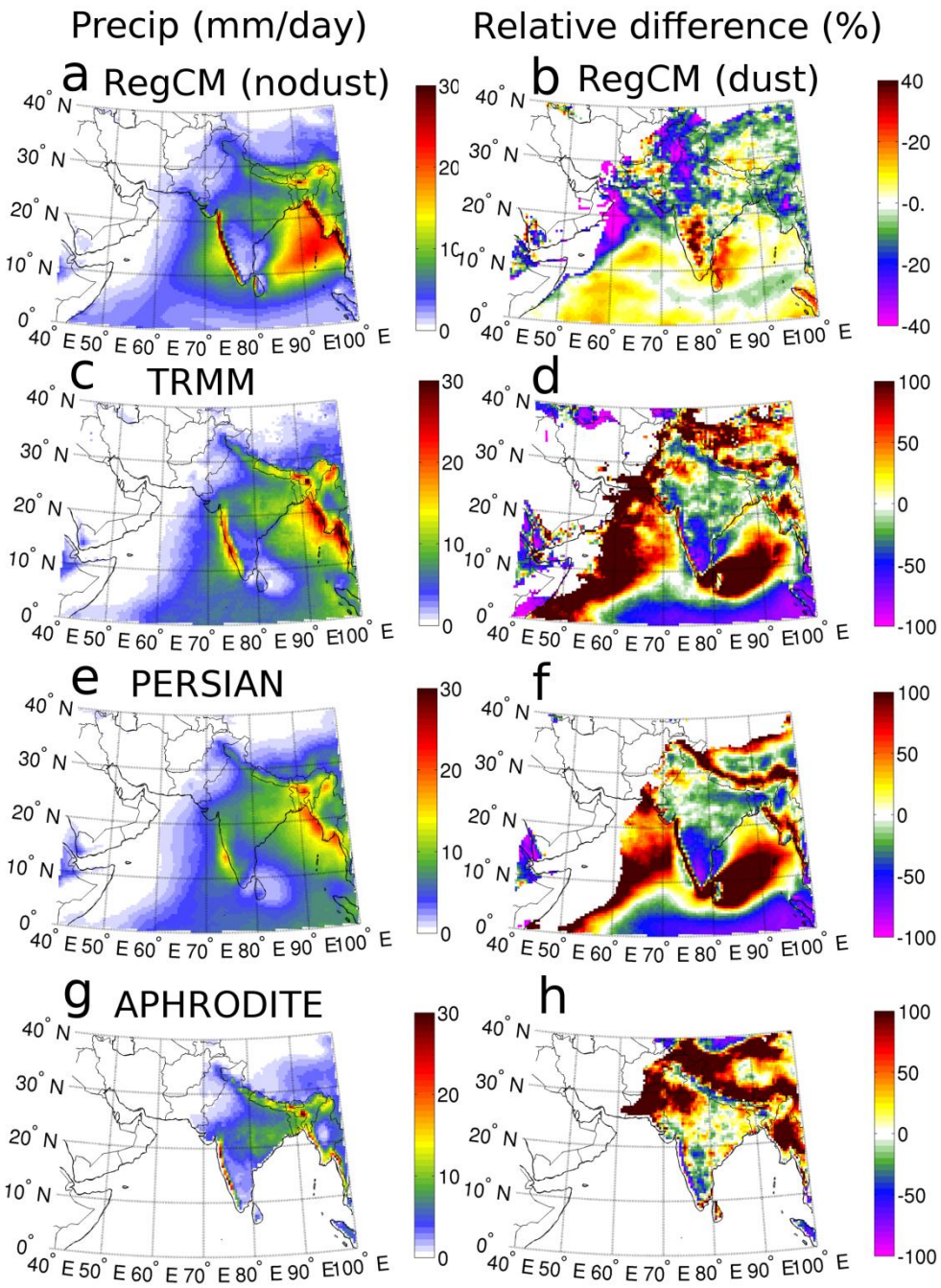
Precip (mm/day)
Relative difference (%)
a RegCM (nodust)
b RegCM (dust)
c TRMM
d
e PERSIAN
f
g APHRODITE
h
40° N
30° N
20° N
10° N
0°
40° E 50° E 60° E 70° E 80° E 90° E 100° E
30
20
10
0
40
-20
-0.
-40
100
50
-50
-100

Figure 7.

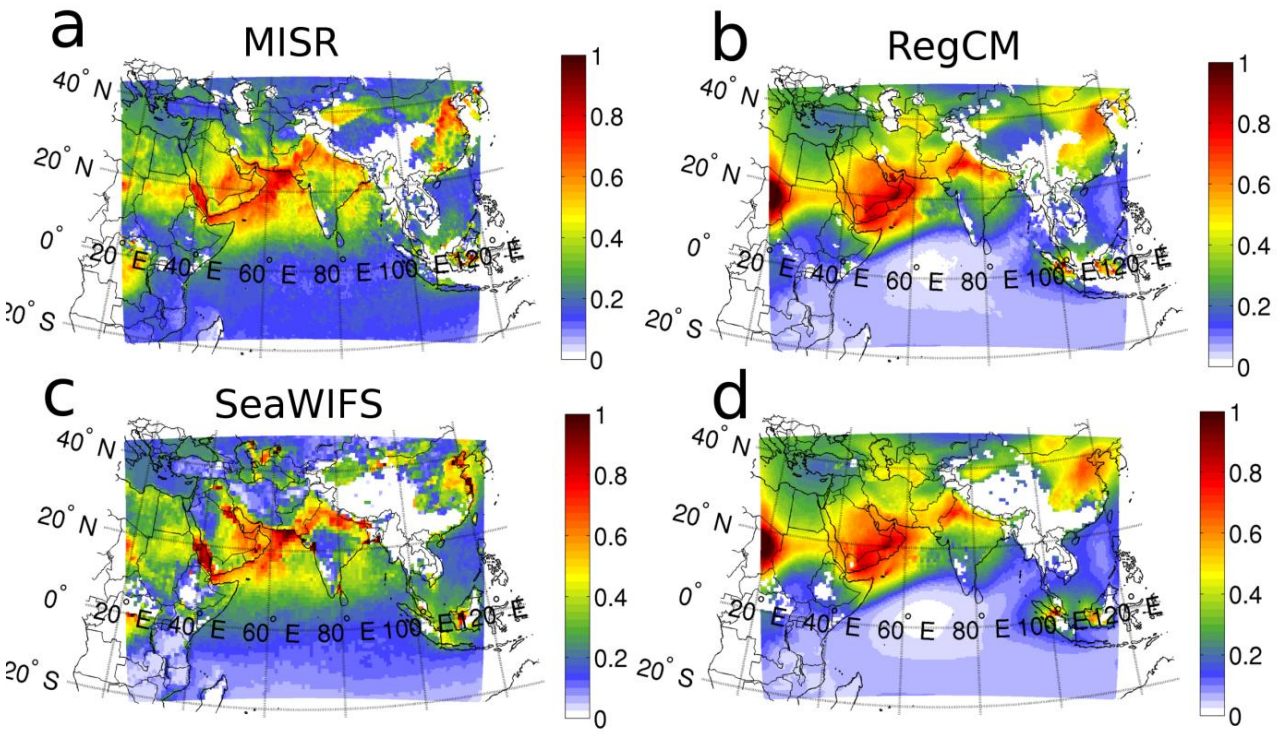
a
MISR
b
RegCM
c
SeaWIFS
d
40° N
20° N
0°
20° S
20° E
40° E
60° E
80° E
100° E
120° E
1
0.8
0.6
0.4
0.2
0

Figure 8

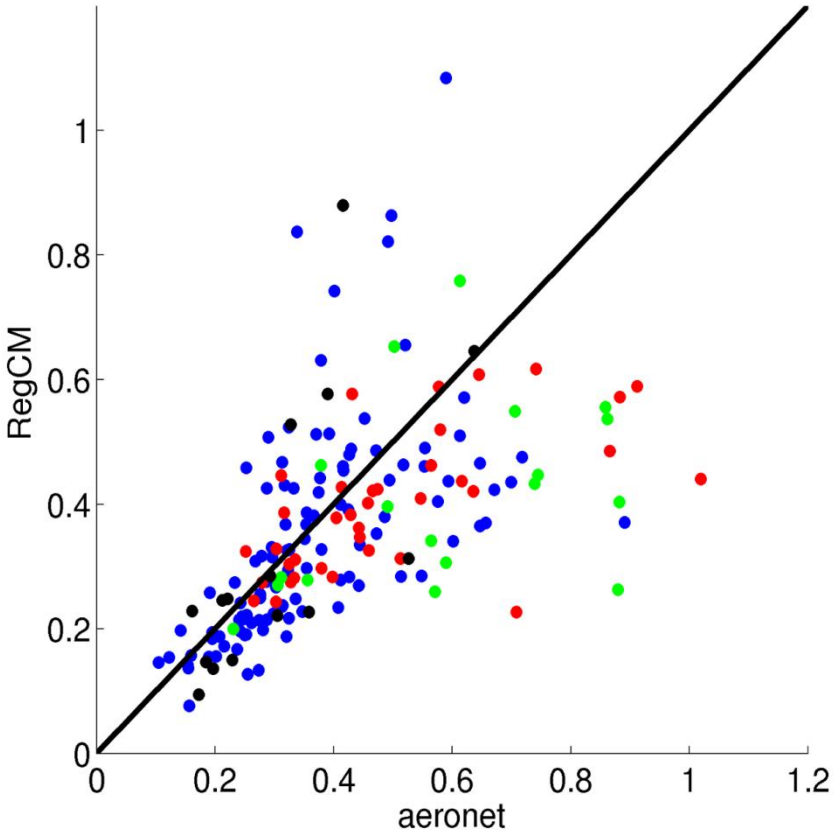

Figure 9.

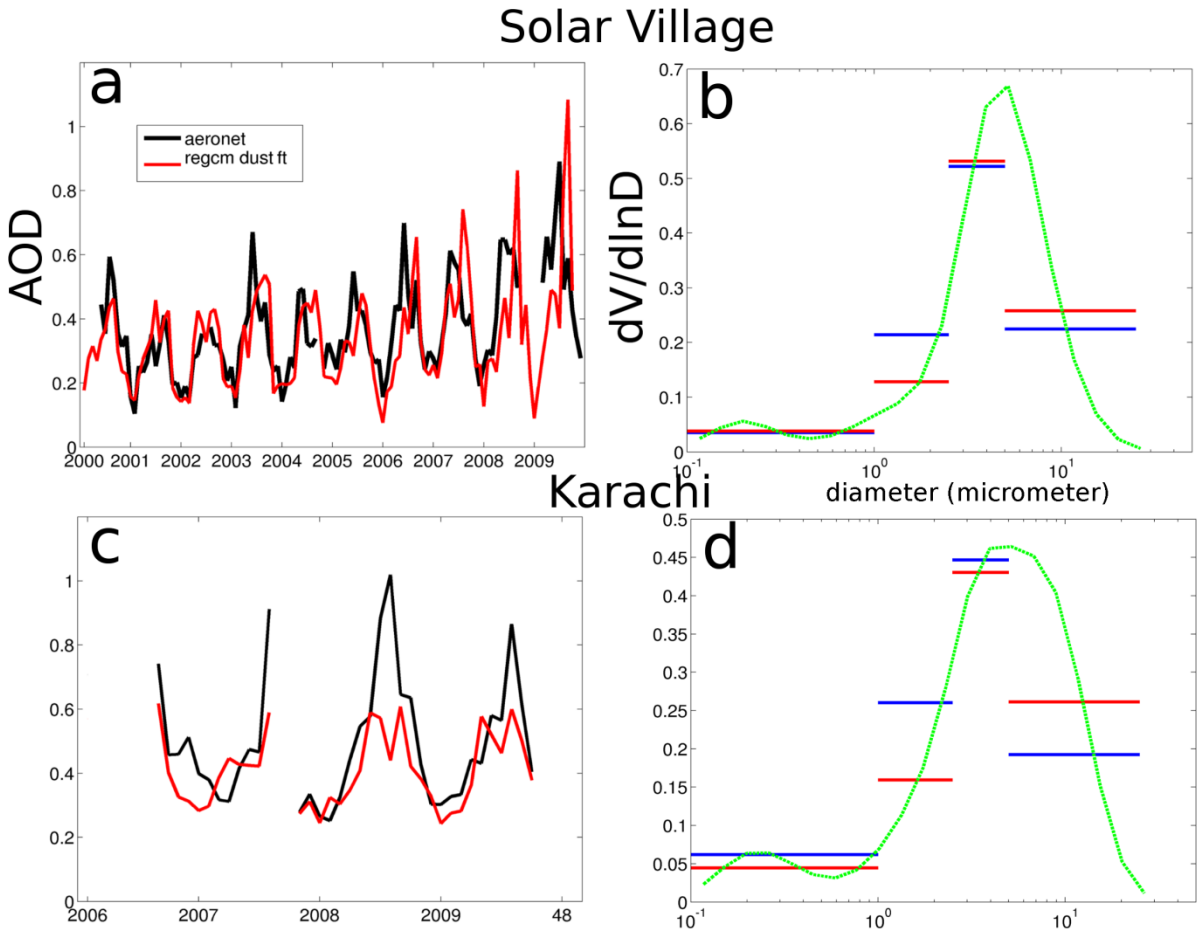
Solar Village
a
aeronet
regcm dust ft
AOD
2000 2001 2002 2003 2004 2005 2006 2007 2008 2009
b
dV/dlnD
diameter (micrometer)
Karachi
c
2006 2007 2008 2009 48
d

Figure 10.

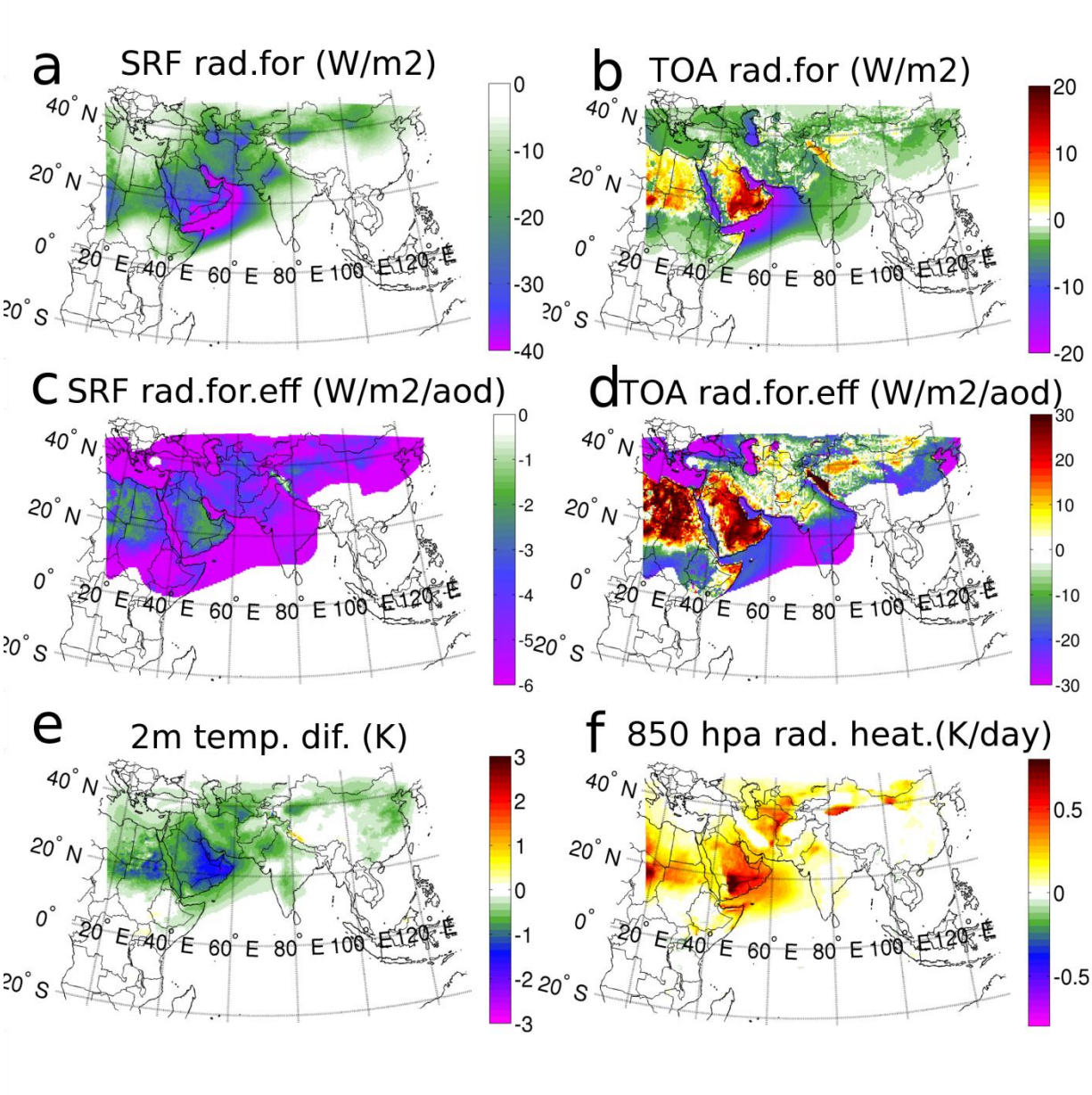
a SRF rad.for (W/m2)
b TOA rad.for (W/m2)
c SRF rad.for.eff (W/m2/aod)
d TOA rad.for.eff (W/m2/aod)
e 2m temp. dif. (K)
f 850 hpa rad. heat.(K/day)
40° N
20° N
0°
20° S
20° E 40° E 60° E 80° E 100° E 120° E

Figure 11.

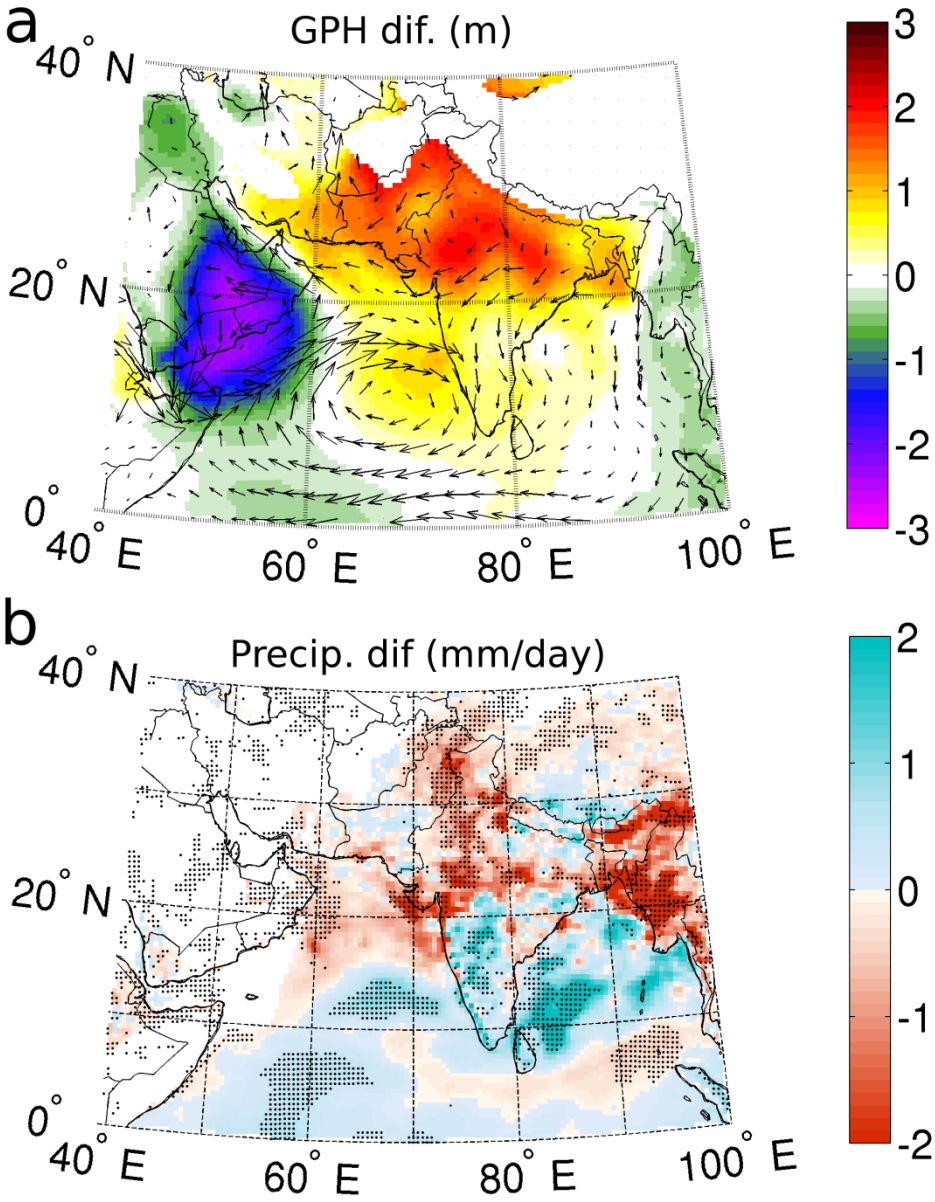
a
GPH dif. (m)
40° N
20° N
0°
40° E
60° E
80° E
100° E
3
2
1
0
-1
-2
-3
b
Precip. dif (mm/day)
40° N
20° N
0°
40° E
60° E
80° E
100° E
2
1
0
-1
-2

Figure 12.

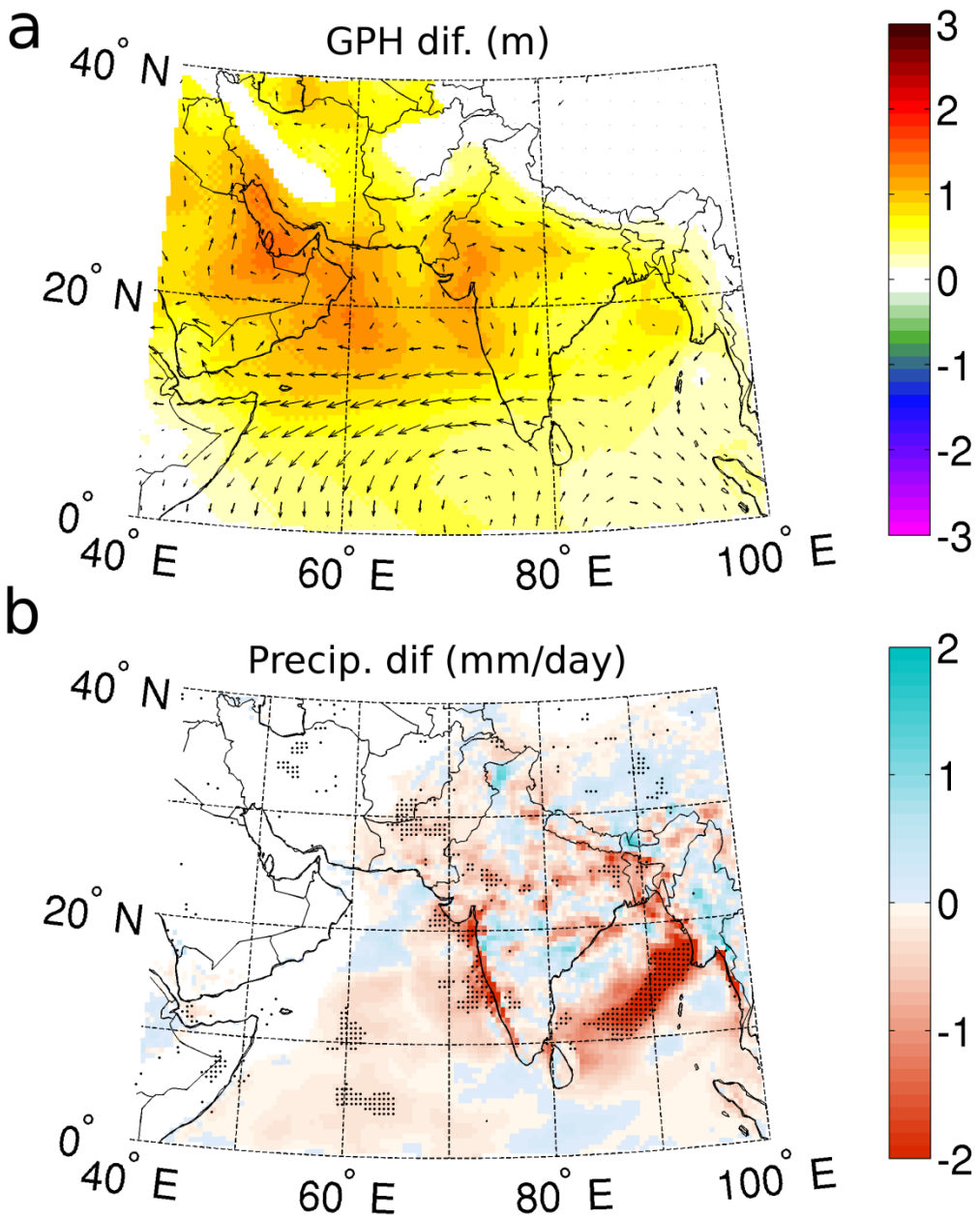
a
GPH dif. (m)
40° N
20° N
0°
40° E
60° E
80° E
100° E
3
2
1
0
-1
-2
-3
b
Precip. dif (mm/day)
40° N
20° N
0°
40° E
60° E
80° E
100° E
2
1
0
-1
-2

1